LUND UNIVERSITY

Disentangling production and climate signals from high-resolution Beryllium records: implications for solar and geomagnetic reconstructions

Zheng, Minjie

2020

Document Version:
Publisher's PDF, also known as Version of record

Link to publication

Citation for published version (APA):
Zheng, M. (2020). *Disentangling production and climate signals from high-resolution Beryllium records: implications for solar and geomagnetic reconstructions*. [Doctoral Thesis (compilation), Department of Geology]. Lund University.

Total number of authors:
1

General rights
Unless other specific re-use rights are stated the following general rights apply:
Copyright and moral rights for the publications made accessible in the public portal are retained by the authors and/or other copyright owners and it is a condition of accessing publications that users recognise and abide by the legal requirements associated with these rights.
• Users may download and print one copy of any publication from the public portal for the purpose of private study or research.
• You may not further distribute the material or use it for any profit-making activity or commercial gain
• You may freely distribute the URL identifying the publication in the public portal

Read more about Creative commons licenses: https://creativecommons.org/licenses/

Take down policy
If you believe that this document breaches copyright please contact us providing details, and we will remove access to the work immediately and investigate your claim.

LUND UNIVERSITY

PO Box 117
221 00 Lund
+46 46-222 00 00

LUNDQUA THESIS 88

Disentangling production and climate signals from high-resolution Beryllium records: implications for solar and geomagnetic reconstructions

MINJIE ZHENG
QUATERNARY SCIENCES | DEPARTMENT OF GEOLOGY | LUND UNIVERSITY 2020

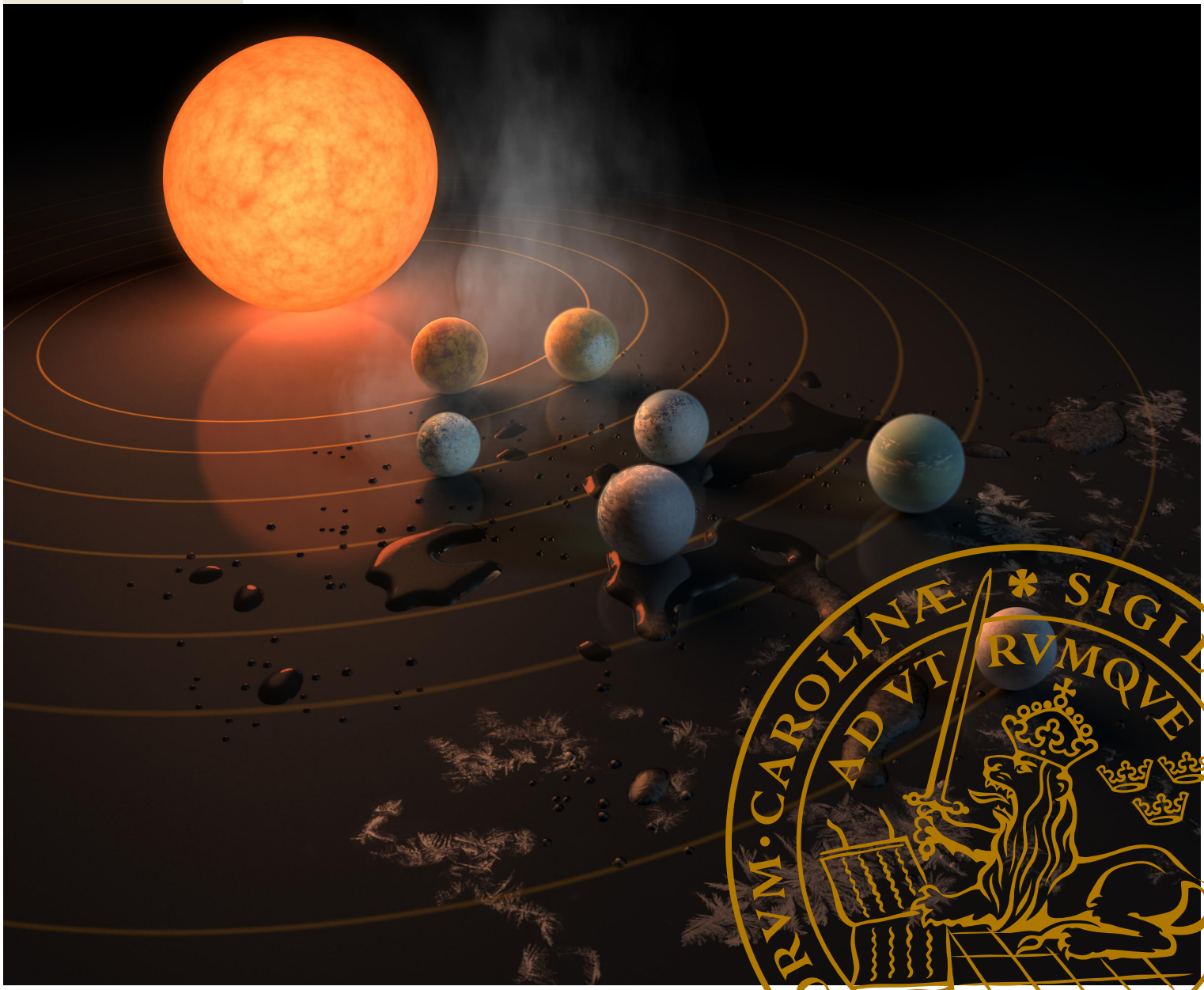

Xiapu, the hometown of the author (Credit: xpsheying.com)

Printed by Media-Tryck, Lund 2020 NORDIC SWAN ECOLABEL 3041 0903

LUND UNIVERSITY

Quaternary Sciences
Department of Geology
Lund University
Sölvegatan 12
SE-223 62 Lund, Sweden
Telephone +46 46 222 78 80

ISSN 0281-3033
ISBN 978-91-87847-50-9

LUNDQUA THESIS 88

Disentangling production and climate signals from high-resolution Beryllium records: implications for solar and geomagnetic reconstructions

Minjie Zheng

LUND
UNIVERSITY

Quaternary Sciences
Department of Geology

DOCTORAL DISSERTATION
by due permission of the Faculty of Science, Lund University, Sweden.
To be defended at Pangea, Department of Geology, Sölvegatan 12, Lund,
on the 8th of October at 9:00.

Faculty opponent
Joel Pedro
University of Tasmania, Australia

Copyright Minjie Zheng

Front cover credit: NASA/Image of the Day

Back cover credit: xpsheying.com

Quaternary Sciences
Department of Geology
Faculty of Science

ISBN: 978-91-87847-50-9 (print)

ISBN: 978-91-87847-51-6 (pdf)

ISSN: 0281-3033

Printed in Sweden by Media-Tryck, Lund University, Lund 2020

Media-Tryck is a Nordic Swan Ecolabel
certified provider of printed material.
Read more about our environmental
work at www.mediatryck.lu.se

MADE IN SWEDEN

Organization

LUND UNIVERSITY
Department of Geology
Sölvegatan 12
SE-223 62 Lund
Sweden

Author: Minjie Zheng

Document name

DOCTORAL DISSERTATION

Date of issue: 4th September 2020

Sponsoring organization

Title: Disentangling production and climate signals from high-resolution Beryllium records: implications for solar and geomagnetic reconstructions

Abstract

The sun is the most important energy source for the Earth's climate system, however, influences of solar variations on climate are not fully understood. Studying past solar activity can improve our understanding of what role the sun plays in Earth's climate. Cosmogenic radionuclides, such as ^{10}Be in ice cores, are powerful tools to reconstruct past solar activity before the period of direct telescope observations. Because the atmospheric production rates of ^{10}Be depend on the strengths of the solar and geomagnetic field, hence measurements of ^{10}Be in ice can provide useful information on variabilities of these two magnetic fields back in time. However, the interpretation of ^{10}Be data is challenged due to the influences of transport and scavenging processes on ^{10}Be from Earth's atmosphere to the natural archives (e.g. ice cores). Unidentified climate imprints on ^{10}Be records could lead to errors in solar and geomagnetic reconstructions.

This project aims to improve our understanding of the climate effects on ^{10}Be through analysis of high-resolution ^{10}Be and ^{7}Be data, in order to improve solar and geomagnetic reconstructions. We present a well-defined seasonally resolved ^{10}Be record for the period 1887-2002 from a NEEM firn core (NEEM07S1) in northwestern Greenland. Through analyzing the sub-annual δ^{18}O records at NEEM site, we identify the seasonal signals with 30% accumulation for November-April (winter) and 70% accumulation for May-October (summer). Both summer and winter ^{10}Be data reflect the production signal induced by solar modulation of galactic cosmic rays. Superimposed on this solar signal we find that the tropopause pressure over 30°N represents an important factor influencing NEEM ^{10}Be concentrations. Summer ^{10}Be concentration, on average, is higher than winter, which could be attributed to the effects of stratospheric intrusion of ^{10}Be. This stratospheric intrusion of beryllium is also supported by the study of weekly-resolved air ^{7}Be records over Europe. Furthermore, by comparing the NEEM ^{10}Be record with other Greenland ^{10}Be records over the last 100 years, we identify that the ^{10}Be values from the Dye3 ice core after 1958 are unusually low, which are resulting from a data quality issue instead of meteorological influences. This period of unusually low Dye3 ^{10}Be values can lead to a normalization problem when connecting radionuclide records to modern levels of solar modulation estimated from neutron monitor data over the past 70 years. We found that disagreements of different solar reconstructions based on Greenland and Antarctica ^{10}Be records can be partly attributed to this data problem. Finally, we present a geomagnetic dipole moment reconstruction for the period from 11.7 ka BP (before present AD 1950) to 108 ka BP based on a new NEEM ^{10}Be record and published GRIP ^{10}Be and ^{36}Cl records. With a first-order correction of cosmogenic radionuclides data using climate proxy data, the "climate correction" results lead to an improved agreement with independent reconstructions compared to simply using radionuclide data. Therefore, with this linear correction method, geomagnetic dipole moment reconstructions based on cosmogenic radionuclides data from ice cores can be extended back in time when there is a strong climate signal in radionuclides data.

Key words: Solar Activity, ^{10}Be, ^{7}Be, ice cores, climate, tropopause, cosmogenic radionuclides, geomagnetic reconstructions, multi-linear regression

Classification system and/or index terms (if any)

Supplementary bibliographical information | Language: English

ISSN and key title: 0281-3033 LUNDQUA THESIS | ISBN: 978-91-87847-50-9

Recipient's notes | Number of pages: 163 | Price

Security classification

I, the undersigned, being the copyright owner of the abstract of the above-mentioned dissertation, hereby grant to all reference sourcespermission to publish and disseminate the abstract of the above-mentioned dissertation.

Signature: 郑敏杰

Date: 4th September 2020

I have no special talent. I am only passionately curious.

---- Albert Einstein

Contents

List of papers

This thesis consists of five papers listed below, which have been attached to the thesis. Paper I and II have been published in journals and are reprinted under permission of the respective publishers. Paper III, IV and V are manuscripts.

Paper I

Zheng, M., Sjolte, J., Adolphi, F., Vinther, B.M., Steen-Larsen, H.C., Popp, T.J., Muscheler, R., 2018. Climate information preserved in seasonal water isotope at NEEM: relationships with temperature, circulation and sea ice. Climate of the Past 14, 1067-1078, doi: 10.5194/cp-14-1067-2018. *Available in open access.*

Paper II

Zheng, M., Adolphi, F., Sjolte, J., Aldahan, A., Possnert, G., Wu, M., Chen, P., Muscheler, R., 2020. Solar and climate signals revealed by seasonal ^{10}Be data from the NEEM ice core project for the neutron monitor period. Earth and Planetary Science Letters 541. 116273, doi: 10.1016/j.epsl.2020.116273. Reprinted with permission from Elsevier

Paper III

Zheng, M., Adolphi, F., Sjolte, J., Aldahan, A., Possnert, G., Wu, M., Chen, P., Muscheler, R., 2020. Solar activity of the past 100 years inferred from ^{10}Be in ice cores – implications for long-term solar activity reconstructions. *(Manuscript)*

Paper IV

Zheng, M., Sturevik-Storm, A., Nilsson, A., Adolphi, F., Aldahan, A., Possnert, G., Muscheler, R., 2020. Reconstruction of the geomagnetic dipole moment variation for the last glacial period based on cosmogenic radionuclides from Greenland ice cores. *In revision, Quaternary Science Reviews.*

Paper V

Zheng, M., Sjolte, J., Adolphi, F., Aldahan, A., Possnert, G., Wu, M., Muscheler, R., 2020. Solar and Meteorological influences on seasonal atmospheric ^{7}Be in Europe for 1975 to 2018. *In revision, Chemosphere.*

Acknowledgements

First of all, my deepest appreciation goes to my main supervisor: Raimund Muscheler who introduced me to this amazing cosmogenic radionuclide world and who shared the excitement of four years of discovery. You always have had your office door open for me and supported me to explore different research topics not planned. You were patient answering my questions and always provided valuable advice when I got lost in projects. I am really grateful for what you have done for me and I truly could not have imaged having a better supervisor for my PhD study.

I would like to thank Florian Adolphi for very constructive comments and advices for manuscripts, well written Matlab scripts and the patience of replying my questions. Jesper Sjolte, thank you for many inspiring discussions with the stable isotope and climate related knowledge. Thank you for the nice trip together in China (and sorry for "stomachache"). Andreas Nilsson is thanked for the geomagnetic filed related discussion and the help when I have problems with *Svensk sammanfattning*. I also want to thank all my co-authors for sharing their knowledge and expertise. A heartfelt thanks to Ala Aldahan for introducing me to Lund and kindly sharing your amazing data, and to Göran Possnert for the help in ^{10}Be measurements. I also want to thank Stefanie Müller for her help in the lab and logistics of samples.

I am grateful to *Chinese scholarship council* for funding this PhD project and to *Kungliga Fysiografiska Sällskapet* for funding the associated research projects.

Doing a PhD abroad is not only about working, but also about making new friends and enjoy the new culture. I have to admit that I am terrible on balancing between work and life. Still, I have met so many great people which I would like to thank for. I would like to thank all my fellow PhD students, both past and present, for making my PhD time fun and interesting. Special thanks to my officemates: Emma, Florian, Sha, Inda, for sharing such a pleasant workplace. I want to especially thank Zhouling, Bingjie and Peng, for inviting me to your many hotpot parties and game nights. Thank you for letting me feel less homesick in Lund. I also want to thank to the rest of the staff at the Department of Geology for all help during my PhD, especially Gert and members of the Kansli that made my PhD life less struggling on computer issues and reimbursements. Many thanks also to the badminton group (Natali, Hans, Mats, Long, Jesper) for every nice Wednesday badminton night.

Many thanks also go to my friends: Mousong, Zhendong, Zhengyao, Yanzi, Zhao and all the others who made my Lund life wonderful. A special thanks to Kenneth Persson for sharing your nice house and bike and being a nice housemate for almost three year. Thanks for showing me the Swedish culture and history and offering me nice beers.

Finally, I would like to give my deepest gratitude to my family and my girlfriend:

最后，我要感谢我的家人和女友。感谢父母的包容和理解，感谢你们在物质和精神上给与我的支持，让我安心在国外完成学业。感谢两个姐姐和姐夫的支持和关心。感谢女友晓静的陪伴和理解，谢谢你最后帮我排版论文格式。感谢你们忍受我最后半年由于论文压力的吐槽。谢谢你们为我做的一切!

1. Introduction

Our knowledge about the solar influence on climate bears large uncertainties (Stocker et al., 2013). Studying past changes in solar activity can assist us understanding what role the sun plays in Earth's climate. However, direct solar observations via telescope only go back to 1610 C.E. (Eddy, 1976) and, therefore, other approaches are required to reconstruct solar activity before direct observations.

Cosmogenic radionuclides, such as ^{10}Be, have been commonly used to reconstruct solar activity for the past centuries and millennia (e.g. Beer et al., 1990; Steinhilber et al., 2012). ^{10}Be is produced by galactic cosmic rays in the upper atmosphere and their flux is modulated by the solar magnetic and geomagnetic field before reaching the atmosphere (Beer et al., 2012). Hence, the production rate of ^{10}Be provides useful information on changes of the solar and geomagnetic activity. After production, ^{10}Be subsequently attaches to aerosols and eventually deposits in natural archives such as ice cores (Beer et al., 2012). Therefore, ^{10}Be in ice cores are a function of the interplay between production, transport and deposition processes. One challenge for applying ^{10}Be in past solar and geomagnetic reconstructions is to separate the production signal from the non-production signal, i.e., transport and deposition processes (hereinafter named as "system effects"). Such system effects, if not corrected, would directly result in errors in solar reconstructions. For example, Usoskin et al. (2003) suggest that the solar activity reaches a distinct maximum during the last 60 years, which is significantly higher than that during the preceding 1000 years. Bard et al. (2000), on the other hand, conclude that solar activity at around 1200 A.D. reaches similar values as present solar activity. Recently, Muscheler et al. (2016) updated the ^{10}Be based solar reconstruction over the last 2000 years and highlight that the difference in Greenland and Antarctic ^{10}Be data can lead to disagreeing conclusions about past solar activity levels (Fig. 1). They suggest that this difference most likely reflects different climate/weather influences on these records for the past 100 years. As the most recent decades are important for normalizing the radionuclide records to modern observations, such differences affect the estimates of solar activity levels further back in time. Additional ^{10}Be records covering this period can help identify the underlying reasons for the difference and contribute to improve reconstructions of past solar activity.

Studying high-resolution (sub-annual) ^{10}Be data from ice cores can provide insights into climate factors governing the ^{10}Be signal that cannot be deciphered by investigating the annual ^{10}Be data only. For example, through comparison of monthly resolution ^{10}Be records to results from a general circulation model (GCM) by Heikkilä et al. (2008a), Pedro et al. (2011a) propose that the stratospheric intrusion of ^{10}Be-enriched air can cause elevated ^{10}Be deposition during late austral summer and early autumn at Law Dome, Antarctica. Sub-annual resolution ^{10}Be data in Greenland are available only for the Dye 3 ice core from 1978 to 1983 (Beer et al., 1991) and the GRIP ice core from 1986 to 1990 (Heikkilä et al., 2008b). These high-resolution ^{10}Be records from Greenland do not span a full solar cycle, making a distinction between climate and production influences on ^{10}Be deposition in Greenland challenging. At the same time, longer ^{10}Be records are the basis for long-term solar activity reconstructions (e.g. Vonmoos et al., 2006).

This thesis aims to address the following aspects:

- To better understand ^{10}Be transport and deposition processes by comparing sub-annual resolution of ^{10}Be and ^{7}Be records with climate data and modelled production rates based on neutron monitor data
- To assess procedures to reduce the climate influence on ^{10}Be records using multi-linear regression models
- To reconstruct the past changes in the geomagnetic field based on cosmogenic radionuclides from Greenland ice cores, after correcting the climate signal in data
- To investigate why two ^{10}Be records (NGRIP and Dye3) from Greenland ice cores showing different decreasing trends over the last 100 years and possible implications for past solar reconstructions

2. Beryllium-10 and beryllium-7

2.1 Atmospheric production

The main cause for ^{10}Be and ^{7}Be production in the Earth's atmosphere are galactic cosmic rays (GCRs, Fig. 2). These highly energetic cosmic particles are composed of protons (~87%), alpha particles (~12%) and heavier nuclei (~1%) (Beer et al., 2012). The particles are charged and are, therefore, influenced by magnetic fields as they travel through the interstellar space. The GCRs are assumed to mainly originate from supernova explosions (Ackermann et al., 2013). By studying radionuclides in meteorites, Vogt et al. (1990) suggest that galactic cosmic ray intensity has been constant within 10% during the last few million years. When the flux of GCRs encounters the heliospheric magnetic field (HMF), the low-energy particles are deflected, leading to a modulation of the low-energy spectrum which depends on the solar magnetic field. Such modulation processes are complicated and usually approximated with a simple modulation function Φ (e.g. Caballero-Lopez, 2004), given by $\Phi=(Ze/A)\phi$, where Z and A are the charge and mass number of the cosmic-ray

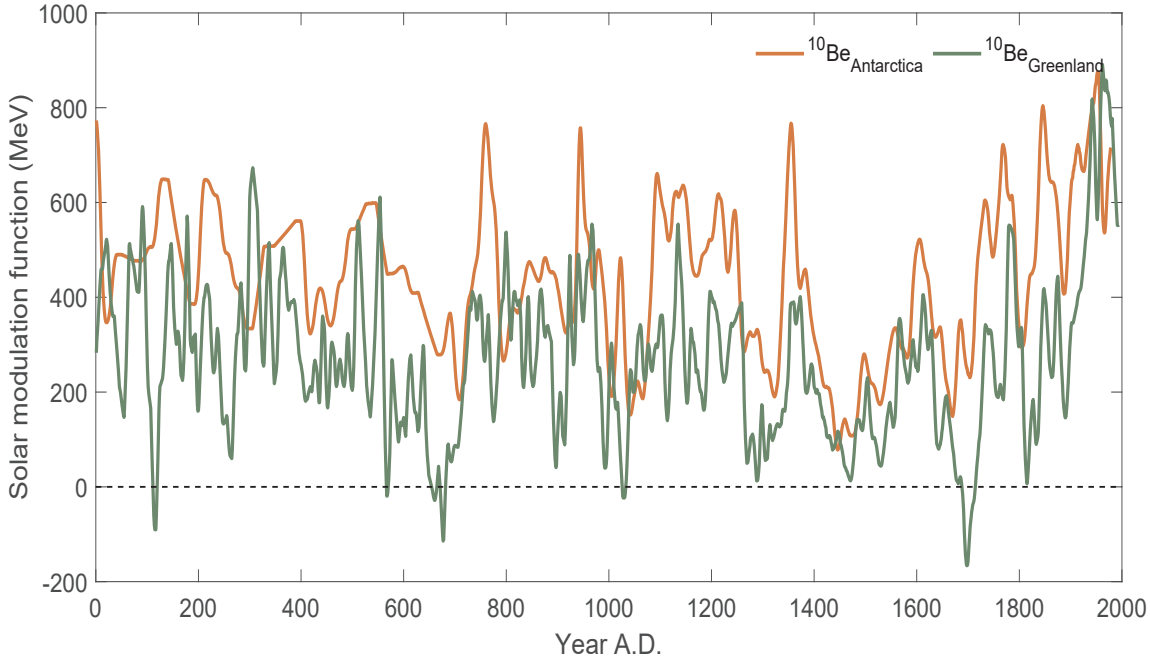

Figure 1. Comparison of solar activity reconstructions based on Greenland and Antarctic ^{10}Be records (modified after Muscheler et al., 2016).

nuclei and ϕ is the solar-modulation parameter, which is directly linked to solar activity. Accordingly, high (low) values of Φ signify strong (weak) magnetic fields enclosed in the solar wind, causing stronger (weaker) deflection of GCRs thus reducing (increasing) the flux of GCRs near the Earth (e.g. Lal and Peters, 1967a).

Before the particles reach the Earth's atmosphere, they also encounter the geomagnetic field which shields the Earth from cosmic rays. Depending on the geomagnetic latitude, the field strength, and the angle of the incident cosmic ray particle the geomagnetic field exerts a rigidity that prevents particles below a cut-off energy from intruding into the atmosphere (e.g. Masarik and Beer, 1999). Once the primary cosmic rays arrive in the Earth's atmosphere, they collide with atmospheric atoms triggering a cascade of nuclear reactions, resulting in the formation of secondary particles (e.g. protons and neutrons). Those secondary particles will further collide with atmospheric atoms leading to the production of cosmogenic radionuclides (Beer et al., 2012; Masarik and Beer, 1999). ^{10}Be and ^{7}Be are produced by spallation reactions during which neutrons and protons collide with the target atoms, nitrogen and oxygen. It should be mentioned that the target atoms do not limit these reactions due to their abundances in the atmosphere. The production reactions of ^{10}Be and ^{7}Be are similar therefore only the main reaction pathways of ^{10}Be are shown:

$$^{14}N+n(p)\rightarrow{}^{10}Be+3p+2n(+4p+n)$$
$$^{16}O+n(p)\rightarrow{}^{10}Be+4p+3n(+5p+2n)$$

Consequently, for a given atmospheric depth, the production rate of atmospheric ^{10}Be and Be relies on the evolution of cosmic showers in the Earth's atmosphere and the number of atmospheric nitrogen and oxygen atoms. The production rate is the lowest at the sea level and increases with the decreasing atmospheric depth (g/cm^2) due to the higher energies of secondary particles therefore more nuclear reactions occur (Fig. 3a). However, from a certain atmospheric depth, the decreasing availability of target atoms compensates the increasing cosmic ray flux, leading to a production peak in the upper troposphere and lower stratosphere. Furthermore, the atmospheric production rate of radionuclides is latitudinal dependent because of the different cut-off rigidities resulting from the geometry of the geomagnetic field (Beer et al., 2012). Therefore, the production rate is higher around the geomagnetic poles and lower in the equatorial region (Fig. 3b). Such latitudinal effects vary in different phases of solar activity. For example, for the strong solar activity (Φ=1000 MeV), the difference of ^{10}Be production rate between polar and equatorial latitude is a factor of 3, while for the case of no solar modulation (Φ=0 MeV), such a latitudinal effect is enhanced to a factor of 7 (Fig. 3b)

Several attempts have been made to model the production rates of cosmogenic radionuclides in the Earth's atmosphere. The first models were empirical and semi-empirical, based on some fragmentary measurements of secondary neutron fluxes in the atmosphere (Lal and Peters, 1967b; O'Brien, 1979). In the 1990s, Masarik and Beer (1999) simulated the cosmic ray propagation in the atmosphere based on a purely physical model including the modulation function Φ and the local interstellar spectrum (LIS), i.e. the particle spectrum outside the heliosphere. Such modern models include all known pro-

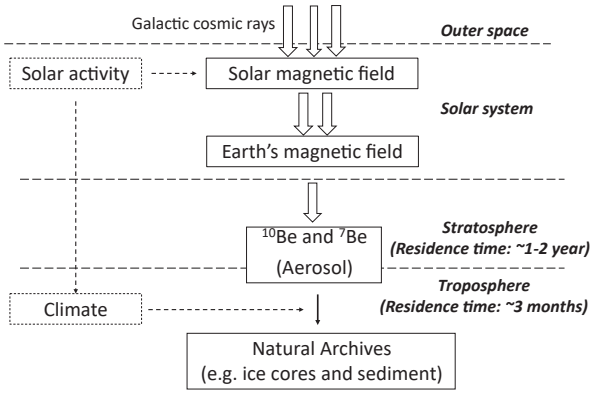

Figure 2. Schematic diagram of ^{7}Be and ^{10}Be atmospheric production and environmental influences (Modified after Muscheler, 2000).

duction processes in the atmosphere and are supposed to estimate the production rates of ^{10}Be and ^{7}Be reasonably well (Kovaltsov and Usoskin, 2010). Nevertheless, there are also noticeable and unresolved differences between the production rate models (e.g. Cauquoin et al., 2014). It should be mentioned that, until the end of 2012, it was impossible to measure the LIS in situ, therefore multiple LIS models exist to describe GCR intensities outside the heliosphere (e.g. Burger et al., 2000; Webber and Higbie, 2010). With Voyager 1 crossing the outer boundary of the solar system at the end of 2012, for the first time an unmodulated LIS below ~500 MeV has been measured (Stone et al., 2013). Based on these measurements, several new LIS models have been published and are included in the calculation of ^{10}Be and ^{7}Be production rates. Some studies (e.g. Poluianov et al., 2016) offer recipes how one can calculate the cosmogenic radionuclides production rates for a given altitude, location and time based on the chosen local interstellar spectrum. This provides a useful tool for integrating the cosmogenic isotope production rates directly into other models, e.g. general circulation models.

Besides the GCRs-induced production, there is also a small amount of ^{10}Be and ^{7}Be formed by solar cosmic rays (SCRs) that originate directly from the Sun. However, SCRs are less energetic than GCRs (e.g. typical energies for GCRs are in the range of ~0.1-10 GeV/nucleon, while for SCRs are in the range of ~1-100 MeV/nucleon, Vogt et al., 1990), and produce less radionuclides per proton. Furthermore, only a small fraction of SCRs exceeds the geomagnetic cut-off rigidity and penetrates the atmosphere. Therefore, the overall contribution of SCRs to the cosmogenic isotope production is negligible (< 1%) (Usoskin et al., 2009; Vogt et al., 1990). However, big solar eruption events can also produce relatively energetic and large particle fluxes resulting in peaks in ^{10}Be records (e.g. Mekhaldi et al., 2015; O'Hare et al., 2019)

2.2 Transport and scavenging processes

After production, ^{10}Be and ^{7}Be attach to aerosols (mainly to sulfate) and are transported in the atmosphere (Igarashi et al., 1998). They behave differently depending on the atmospheric layer they are produced in. Globally, 60-70% of the columnar ^{10}Be and ^{7}Be production occurs in the stratosphere, and the rest in the troposphere (Fig. 4). The stratosphere has a rather stable stratification with less vertical transport than in the troposphere. It also contains lower water vapor concentration than the troposphere and, therefore, little precipitation occurs in stratosphere. These differences are reflected in the residence time of ^{10}Be and ^{7}Be in these two layers. Observational and modelling studies report atmospheric ^{10}Be residence times of about 1 year in the stratosphere and several weeks in the troposphere before deposition (e.g. Heikkilä et al., 2009; Raisbeck et al., 1981). The long residence time in the stratosphere allows for latitudinal mixing of ^{10}Be and smoothing out the effect of latitudinal production differences. Therefore, the ^{10}Be deposited at any given latitude is usually considered as proportional to

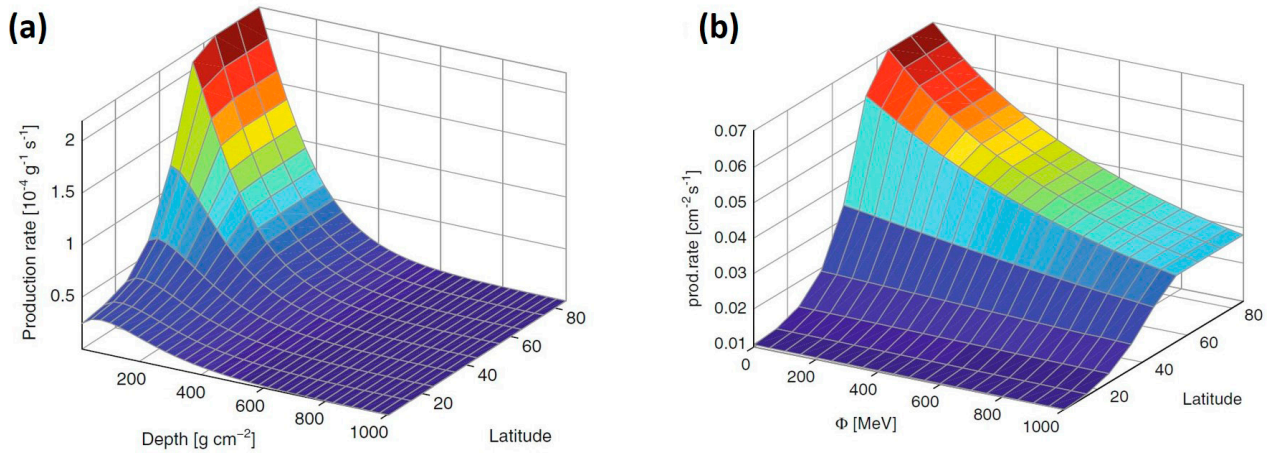

Figure 3. (a) Dependence of ^{10}Be production rates given as ratio to airmass on atmospheric depths and geomagnetic latitudes for the present-day geomagnetic field. (b) Dependence of ^{10}Be production rates upon geomagnetic latitudes and solar modulations for the present-day geomagnetic field. (Modified after Beer et al., 2012)

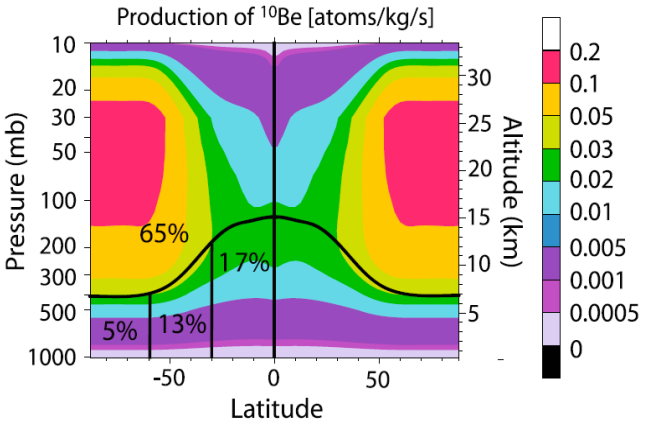

Figure 4. Distribution of the ^{10}Be production rate in the atmosphere at Φ =700 MeV and present-day geomagnetic dipole moment. The black line shows roughly the location of the tropopause and the percentages indicate the amount of ^{10}Be produced in that atmospheric compartment. The latitude is divided into three regions: 0–30°, 30°–60° and 60°–90° roughly following the atmospheric circulation structure (Heikkilä et al., 2008a).

the relative changes in global mean production rate, not the local production rate. The ^{10}Be deposition in polar regions, for instance, is usually assumed as proportional to the relative changes in global averaged production rate, because the major part of the ^{10}Be deposition (~65%) has been suggested to arise from the stratosphere where the ^{10}Be is well mixed (Heikkilä et al., 2009). Due to its short half-life time (53.3 days), ^{7}Be in the stratosphere is not as well mixed as ^{10}Be. Furthermore, ^{7}Be produced at altitudes higher than 20 km is largely decayed before getting transported to the troposphere (Delaygue et al., 2015).

The tropopause (defined as the atmosphere layer between the troposphere and stratosphere where the temperature decreasing rate lower than 2 K km^{-1}; World Meteorological Organization, 1992) is the boundary between troposphere and stratosphere, which acts as a barrier limiting ^{10}Be and ^{7}Be transport between these two atmospheric layers. The height of the tropopause is latitudinally and seasonally variable which influences ^{10}Be and ^{7}Be deposition on a regional scale. For example, at the equator, ~40% of the ^{10}Be production happens in the stratosphere while at the poles ~90% production happens in the stratosphere (Fig. 4) due to the low geomagnetic cut-off rigidity (i.e. more lower energy particles contributing to the high altitude production) and the lower tropopause height in the polar region compare to the tropics (Heikkilä et al., 2008a). Besides the latitudinal dependence, seasonal variations of the tropopause height can also affect the ^{10}Be and ^{7}Be deposition processes via, for example, direct input of ^{10}Be from stratosphere to the troposphere in the austral summer-autumn in Antarctica (e.g. Pedro et al., 2011b). Usually, for an aerosol particle to get through the tropopause it has to grow sufficiently large (e.g. r > 0.05 μm; Heikkilä, 2007) for gravitational settling to begin. Another way of exchange between these layers is the transport along isentropic or constant potential temperature surfaces (Beer et al., 2012). An air parcel can move along these surfaces neither gaining nor losing energy. The isentropic lines cross the tropopause at mid-latitudes, the so-called "tropopause breaks", providing a gate across the tropopause barrier. This "gate" and relatively high local precipitation cause the high deposition of ^{10}Be at mid-latitudes (Fig. 5).

Once ^{10}Be and ^{7}Be are produced or transported to the troposphere, they will be removed within days or weeks by scavenging processes which include dry and wet depositions. Wet deposition describes the deposition of aerosols through scavenging by precipitation. Wet deposition is regarded as the most efficient removal process of ^{10}Be and ^{7}Be (Beer et al., 2012). As one can see from the Figure 5, high ^{10}Be deposition rates occur where the precipitation is high and low ^{10}Be deposition rates occur where

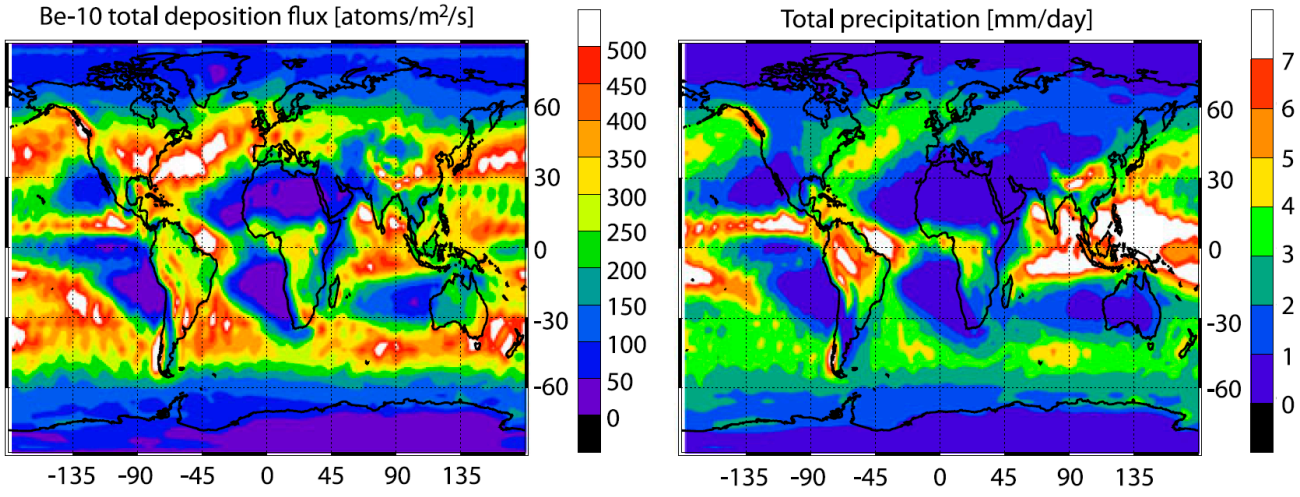

Figure 5. Deposition flux of ^{10}Be, modelled with the ECHAM5-HAM general circulation model, averaged over 1986–1990 (a) and the precipitation rate for the same period (b) (Heikkilä et al., 2008a).

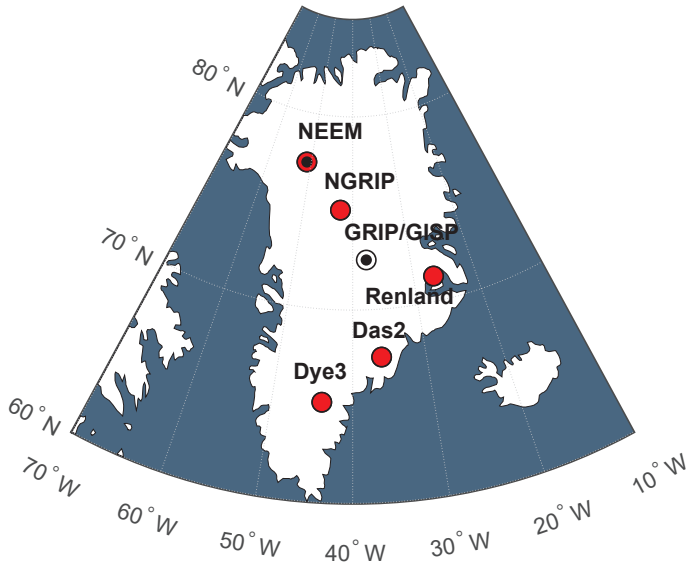

Figure 6. Locations of drilling sites in Greenland with ^{10}Be records available for the neutron monitor period (red) and for the last glacial period (black dot).

the precipitation is low. In contrast to wet deposition, dry deposition means that aerosol particles deposit without scavenging through precipitation. Dry deposition usually dominates in areas that have dry climate such as central Antarctica and other deserts.

Changes between dry and wet deposition of ^{10}Be have to be accounted for in the interpretation of ^{10}Be records. In practice, the ice concentration of ^{10}Be is the measurement of ^{10}Be in a sample which reflects the number of atoms per gram of the sample material. For ice cores this is determined by the number of atoms deposited at the sampling site in relation to the snow accumulation rate. Consequently, if deposition occurred entirely in a dry mode, precipitation would dilute the deposited ^{10}Be concentration. For example, Wagner et al. (2001b) observe a roughly halved ^{10}Be concentration for periods of doubled accumulation rates during the Marine Isotope Stage 3 (MIS-3) in GRIP and GISP2 ice cores. In such a case, it is more appropriate to use the ^{10}Be flux (the concentration multiplied with accumulation and ice density) than the concentration because flux indicates the deposition rate of ^{10}Be atoms per unit area and time. On the other hand, if ^{10}Be was entirely deposited in a wet mode, the ^{10}Be flux would increase with precipitation rates and hence, the ^{10}Be concentration is independent from snow accumulation rate and proportional to the local atmospheric concentration (Alley et al., 1995). In reality both dry and wet deposition processes usually occur together over Greenland (Alley et al., 1995). Whether to use ^{10}Be concentration or flux as an approximation of production signal depends on the specific situation. In general, if the precipitation changes occur on local and regional scales, then the concentration is the better choice for the measures of the production signal. However, when climate changes occurred on large scales (e.g. hemisphere or global) then fluxes are usually preferable (e.g. MIS-3 period). In the first case, concentrations are often similar to fluxes and both concentrations and fluxes will lead to similar results (Beer et al., 2012).

There are different approaches to deal with climate effects on ^{10}Be deposited in polar regions. One way is to average ^{10}Be records from different ice cores or use principal component analysis (e.g. Abreu et al., 2012; Steinhilber et al., 2012) to extract the common production signal of ^{10}Be. Other studies compare ^{10}Be to another cosmogenic radionuclide ^{14}C that is produced in a similar way as ^{10}Be in the atmosphere. ^{14}C oxidizes to $^{14}CO_2$ after production, joins in the carbon cycle and hence behaves completely differently compared to ^{10}Be. Comparing these two radionuclides can help to extract the common production signal (e.g. Adolphi et al., 2014; Steinhilber et al., 2012). Another way is to use general circulation models (GCMs) to study the climate effects in a theoretical approach. Two GCMs have been used to simulate the ^{10}Be transport processes: ModelE (Field and Schmidt, 2009; Field et al., 2006) and ECHAM5-HAM (Heikkilä et al., 2008a; Heikkilä et al., 2008b). However, some disagreements still exist between these model results. For example, the result of ModelE has detected a latitudinal bias on the ^{10}Be depositions response to production changes (Field et al., 2006) while the ECHAM5-HAM results show no such a bias (Heikkila et al., 2009).

3. Materials and methods

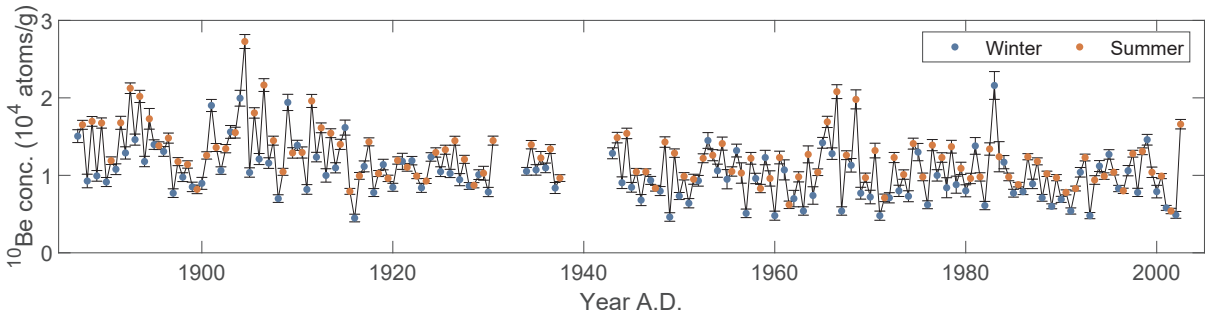

Figure 7. NEEM ^{10}Be concentrations for 1887-2002 presented in Paper II and III together with their measurement uncertainties. Summer values are indicated in red, while winter concentrations are shown in blue.

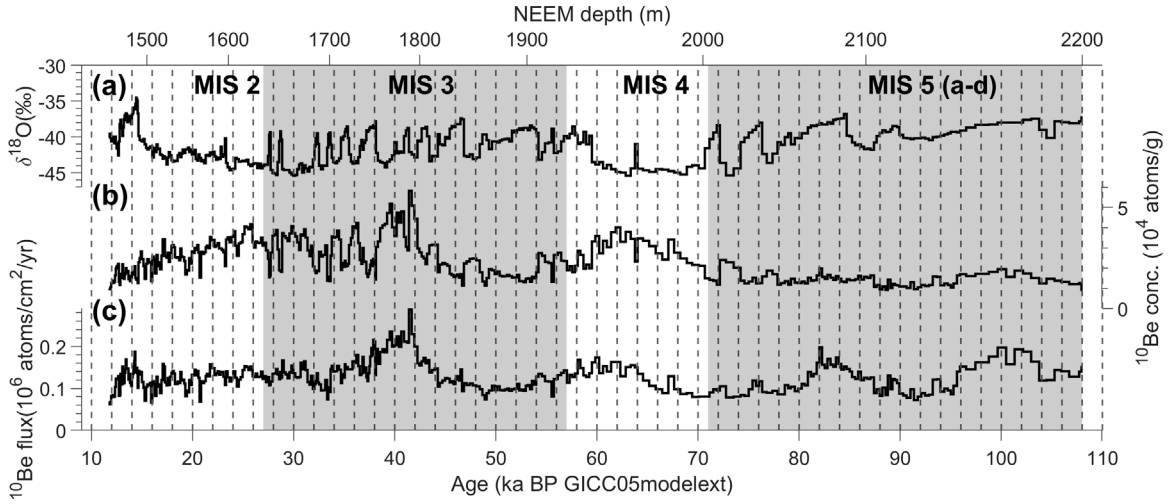

Figure 8. δ^{18}O and ^{10}Be concentrations/fluxes from the NEEM ice core for 11.7-108 ka BP. (a) NEEM δ^{18}O data (NEEM community members, 2013; Schupbach et al., 2018). (b) NEEM ^{10}Be concentrations. (c) NEEM ^{10}Be fluxes calculated by multiplying the concentration of each sample with the corresponding accumulation rate and ice density. MIS indicates the marine isotope stage.

3.1 NEEM ^{10}Be records

Two new ^{10}Be records related to the NEEM project (The North Greenland Eemian Ice Drilling) are of fundamental importance for this thesis (Paper II, III and IV). The chemical preparation of these samples is described in the following section 3.2. The main NEEM project aim was to retrieve a deep ice core record spanning back to the last interglacial period from Northwest Greenland during 2007-2012 (Fig. 6, 77.45° N, 51.06° W, 2450 m.a.s.l., NEEM community members, 2013). To assist interpreting the climate proxy records along the deep ice core, several shallow firn/ice cores were also drilled around the camp as part of the program.

The first NEEM ^{10}Be record is obtained from such a short firn core (NEEM07S1) covering the period 1887-2002 with well-defined winter and summer ^{10}Be (Fig. 7). To identify the seasonal signal in this core, four sub-annual NEEM δ^{18}O data sets over the last 150 years from Masson-Delmotte et al. (2015) are used (Paper I). Unfortunately, ice samples of the years 1931-1933 and 1938-1942 were missing and could not be found at the ice storage facility at Copenhagen University. This new seasonally resolved ^{10}Be record is a key to assess the weather/climate influence on ^{10}Be during winter and summer seasons (Paper II), and to investigate the possible reason(s) for the inconsistencies of the two previous published ^{10}Be records (Dye3 and NGRIP) showing different trends over the last 100 years (Paper III).

The second NEEM ^{10}Be record is obtained from the NEEM deep core covering the period 11.7 ka -108 ka BP (Fig. 8) The temporal resolution ranges from 54 years per sample to 1329 years with an average resolution of 237 years/sample for the 11.7-108 ka BP period. The ice samples came from bandsaw dust (homogenously mixed) gathered from when the NEEM deep ice core was cut along the length. The ^{10}Be measurement of the sawdust samples is a new approach to obtain a continuous ^{10}Be record without requiring sampling the ice core itself (Sturevik-Storm et al., 2014). Together with the published ^{10}Be (Adolphi et al., 2014; Muscheler et al., 2004; Wagner et al., 2001a; Yiou et al., 1997) and ^{36}Cl records (Baumgartner et al., 1998; Wagner et al., 2000) from the GRIP ice core we extend the radionuclides-based geomagnetic dipole moment reconstruction to 108 ka BP, after applying a climate correction on the radionuclide

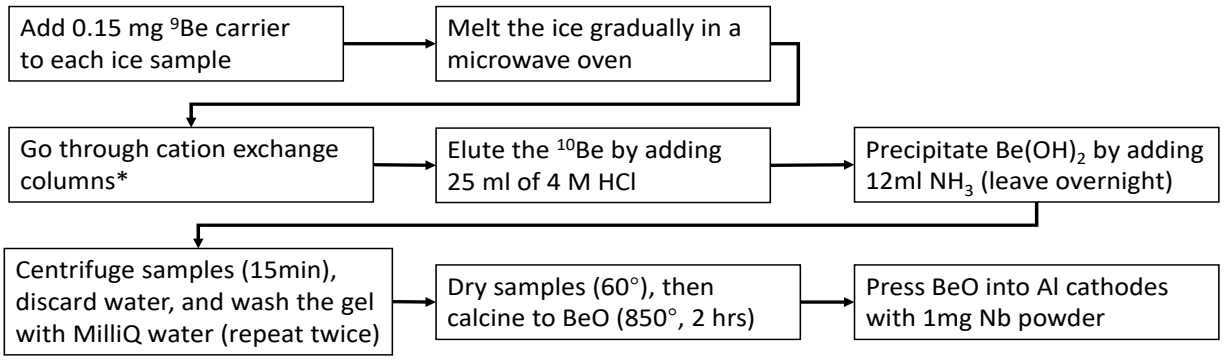

Figure 9. Flowchart showing the procedure for extracting the ^{10}Be from ice samples for AMS measurements. *denotes as Bio-Rad Poly-Prep® prefilled chromatography cation columns AG 50W-X8 resin 100-200 mesh hydrogen form 0.8x4 cm.

data (Paper IV).

3.2 Preparing ice core ^{10}Be samples

The chemical preparation to extract NEEM ^{10}Be from ice samples is shown in Fig. 9, following the procedure by Sturevik-Storm et al. (2014). Ice samples were prepared at the Radionuclide laboratory at Lund University (Paper II-III) and the ^{10}Be laboratory at Uppsala University (Paper IV). All ^{10}Be samples were measured at the Accelerator Mass Spectrometry (AMS) facility of the Tandem laboratory at Uppsala University. Several blanks consisting of 200 g of MilliQ water were processed in the same procedure to estimate the background value for ^{10}Be measurements.

First 0.15 mg ^{9}Be carrier was added to the ice sample. The measurement of the ^{10}Be/^{9}Be ratio avoids effects due to losing samples during preparation. Subsequently, samples were gradually melted in a microwave oven and filled into clean and dry plastic bags. These bags are connected to ion exchange columns via silicone tubes and the ice water is passed through ion exchange columns. 25ml of 4M HCL was added through open quartz tubes to extract ^{10}Be from the resin. 12ml ammonia was then added to form the beryllium hydroxide, $Be(OH)_2$. Tubes were left overnight to ensure a complete formation of $Be(OH)_2$. The precipitate $Be(OH)_2$ was centrifuged to separate the gel-like hydroxide at the bottom of tubes. The $Be(OH)_2$ gel was thereafter transferred to the small centrifuge tubes with Milli-Q water added. After completely mixing the gel with Milli-Q water, the small tubes were centrifuged again. These steps were done twice to make sure only $Be(OH)_2$ gel was left. Samples thereafter were heated in the oven to oxidize beryllium to BeO. The oven temperature was slowly increased to 850°C and kept at this temperature for 2 hours. Finally, about 1 mg of niobium (Nb) was added to each BeO sample and the mixture was pressed into target holders (Al cathodes) to facilitate AMS measurements. The ^{10}Be concentration (atoms/g) of each sample is calculated as the following equation (Berggren, 2009):

$$^{10}\text{Be conc} = R/R_{st} \times \text{standard} \times W_c/W_s \times N_A/A_r$$

Where R/R_{st} is the measured ratio of ^{10}Be counts over ^{9}Be counts. Standard is the standard ratio of ^{10}Be and ^{9}Be (University of California Berkeley ^{10}Be standard ID 14-5-5, ^{10}Be/^{9}Be =2.502 $\times 10^{-11}$) (Nishiizumi et al., 2007). W_c and W_s are the weight of carrier ^{9}Be and ice samples, respectively. N_A is the Avogadro constant (6.022×10^{23} atoms mol^{-1}) and A_r is the atomic weight of beryllium (9.01 g mol^{-1}).

4. Summary of papers

This thesis is based on the compilation of 5 papers with the objective of assessing the climate influences on beryllium and minimizing such climate influences from ^{10}Be records in ice cores. Contributions of authors to each of the following papers are shown in Table 1.

Paper I

Zheng, M., Sjolte, J., Adolphi, F., Vinther, B.M., Steen-Larsen, H.C., Popp, T.J., Muscheler, R., 2018. Climate information preserved in seasonal water isotope at NEEM: relationships with temperature, circulation and sea ice. Climate of the Past 14, 1067-1078, doi: 10.5194/cp-14-1067-2018.

To obtain the seasonally resolved ^{10}Be data, it is necessary to identify the seasonal signal in the ice core. To achieve this, we analyze the sub-annually resolved $\delta^{18}O$ records from four shallow NEEM firn cores covering the last 150 years. We followed the method by Vinther et al. (2010) through analyzing correlations between NEEM $\delta^{18}O$ and observed temperature data. Based on correlation analysis, we attribute about 70% and 30 % of annual accumulation of firn core to summer (May-October) and winter (November-April) respectively. An example of the definition of summer and winter seasons in the NEEM07S1 ice core is shown in Figure 10. We only

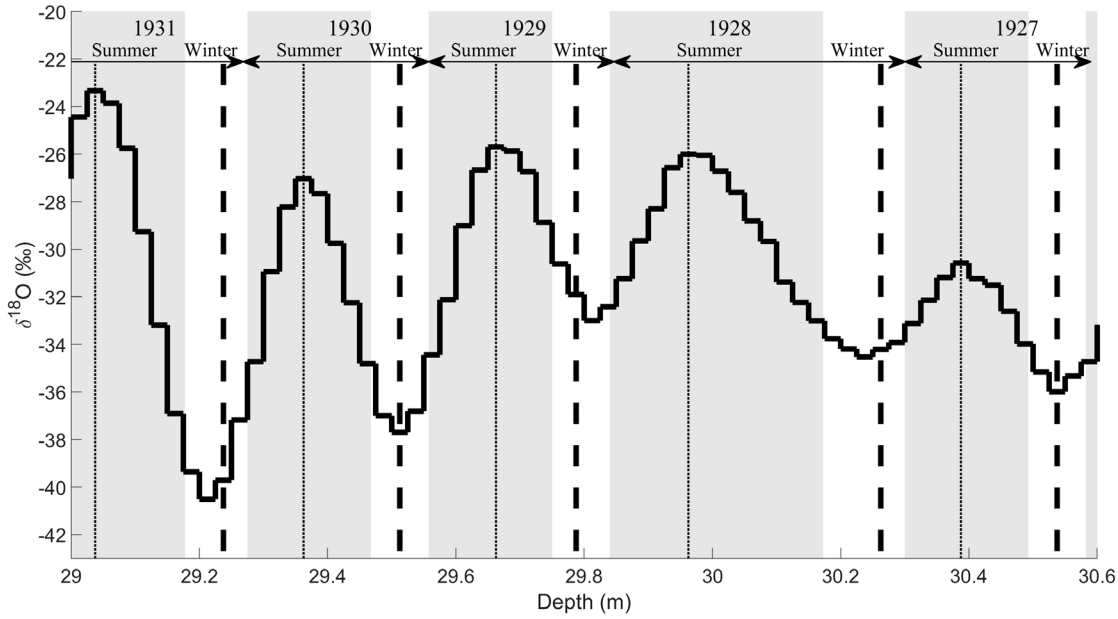

Figure 10. An example of dating and definition of summer and winter seasons in the NEEM07S1 ice core based on a 70% summer and 30% winter deposit fraction center on the appropriate season. The dashed lines are the depth of the onset of annual layers defined by Masson-Delmotte et al. (2015). The dotted lines are the depth where $\delta^{18}O$ reaches the maxima within the year.

distinguish the winter and summer seasons as it is very hard to reliably pinpoint the spring and autumn in $\delta^{18}O$ records. We found that the NEEM summer $\delta^{18}O$ signal correlates strongly with summer western Greenland coastal temperature while no significant correlations between NEEM winter $\delta^{18}O$ data and western Greenland coastal winter temperature are observed. The strong footprint of temperature in NEEM summer $\delta^{18}O$ record suggests that the summer $\delta^{18}O$ record, rather than the winter $\delta^{18}O$ record, is a better temperature proxy at the NEEM site. The NEEM winter $\delta^{18}O$ is found to be highly correlated with Baffin Bay sea ice concentration (SIC) for the period 1901-2004. The NEEM winter $\delta^{18}O$ may reflect sea ice variations in Baffin Bay rather than temperature itself. In addition, despite a dominant signal of North Atlantic Oscillation (NAO) in the central-southern Greenland ice core $\delta^{18}O$ data, the NAO pattern exerts a weak influence on NEEM seasonal $\delta^{18}O$ variations. This has to be kept in mind when combining NEEM $\delta^{18}O$ records with other proxy data in circulation reconstructions.

Paper II

Zheng, M., Adolphi, F., Sjolte, J., Aldahan, A., Possnert, G., Wu, M., Chen, P., Muscheler, R., 2020. Solar and climate signals revealed by seasonal ^{10}Be data from the NEEM ice core project for the neutron monitor period. Earth and Planetary Science Letters 541. 116273, doi: 10.1016/j.epsl.2020.116273.

The high-resolution ^{10}Be data longer than one full solar cycle (11-year) enable a quantification of the influences of atmospheric circulation and deposition processes on the ^{10}Be signal in ice. Based on results of the paper I, we obtain a seasonally resolved ^{10}Be record from the NEEM firn core (NEEM07S1) located in the northwestern Greenland over the neutron monitor period (1951-2002). The results suggest that both summer and winter ^{10}Be reflect the production signal induced by solar modulation of galactic cosmic rays. However, superimposed on this solar signal we find that the tropopause pressure over 30°N represents an important factor influencing NEEM ^{10}Be concentrations on seasonal and annual scales. Summer ^{10}Be also correlates significantly with the tropopause pressure over Greenland suggesting a direct contribution of stratospheric ^{10}Be during summer to the ^{10}Be deposition in Greenland. To correct for these transport/deposition influences, we apply a first-order correction to the ^{10}Be data using a multi-linear regression model. The "climate-corrected" ^{10}Be record shows a comparable skill for reconstructing production rate changes as the stacking method that averaging ^{10}Be records from five different ice cores in Greenland. The results suggest that the correction approach can be a complementary method to the stacking to better isolate the production rate signal from the ^{10}Be data when only limited data are available.

Paper III

Zheng, M., Adolphi, F., Sjolte, J., Aldahan, A., Possnert, G., Wu, M., Chen, P., Muscheler, R., 2020. Solar activity of the past 100 years inferred from ^{10}Be in ice cores – implications for long-term solar activity reconstructions. (Manuscript)

Table 1. Author contributions

	Paper I	*Paper II*	*Paper III*	*Paper IV*	*Paper V*
Study design	J. Sjolte M. Zheng R. Muscheler	R. Muscheler M. Zheng F. Adolphi	M. Zheng R. Muscheler	R. Muscheler M. Zheng A. Aldahan	M. Zheng A. Aldahan R. Muscheler
^{10}Be preparation and measurements	-	M. Zheng G. Possnert P. Chen	M. Zheng G. Possnert	A. Sturevik-Storm G. Possnert	-
Data analysis	M. Zheng J. Sjolte	M. Zheng F. Adolphi	M. Zheng	M. Zheng	M. Zheng
Data interpretation and discussion	M. Zheng J. Sjolte R. Muscheler F. Adolphi B. Vinther H. Steen-Larsen	M. Zheng R. Muscheler F. Adolphi J. Sjolte A. Aldahan M.Wu	M. Zheng R. Muscheler F. Adolphi J. Sjolte A. Aldahan M. Wu P. Chen	M. Zheng R. Muscheler A. Nilsson F. Adolphi A. Sturevik-Storm A. Aldahan	M. Zheng R. Muscheler J. Sjolte F. Adolphi A. Aldahan M. Wu G. Possnert
Writing	M. Zheng	M. Zheng	M. Zheng	M. Zheng	M. Zheng
Comments on manuscript	All co-authors	All co-authors	All co-authors	All co-authors	All co-authors

Two ^{10}Be records (Dye3 and NGRIP ice cores) from Greenland ice cores show different decreasing trends (-5.8%/decade for Dye3 and -3.5%/decade for NGRIP) over the last 100 years. This difference can lead to different conclusions about past changes in solar activity. However, the reasons behind this disagreement remains unresolved. In paper III we analyze the NEEM seasonally resolved ^{10}Be record for the period 1887-2002 with new measurements (1887-1950) completing the NEEM record (1951-2002) from paper II. We observe the summer ^{10}Be concentration in the NEEM record to be higher than the winter concentration, which can be attributed to the stratospheric ^{10}Be intrusions in summer. Summer ^{10}Be shows the similar significant decreasing trend (-2.9%/decade) as winter (-2.85%/decade) for the period 1887-2002. By comparing the NEEM data to ^{10}Be data from the NGRIP and Dye3 ice cores from Greenland we identify that the Dye3 ^{10}Be data for 1958-1985 is significantly lower. By excluding the Dye3 ^{10}Be data after 1958, differences between solar reconstructions based on Greenland and Antarctic ^{10}Be data over last 2000 years are strongly reduced. This suggests that future solar reconstructions should carefully assess such systematic differences between different ^{10}Be records, especially when connecting the radionuclide variations to the absolute solar modulation estimates reconstructed from the neutron monitor data.

Paper IV

Zheng, M., Sturevik-Storm, A., Nilsson, A., Adolphi, F., Aldahan, A., Possnert, G., Muscheler, R., 2020. Reconstruction of the geomagnetic dipole moment variation for the last glacial period based on cosmogenic radionuclides from Greenland ice cores. In revision, Quaternary Science Reviews.

Cosmogenic radionuclide records from ice cores can be used to reconstruct past changes in the geomagnetic dipole moment (GDM) because changes in cosmogenic radionuclide production rates are linked to GDM variations (e.g. Muscheler et al., 2005; Wagner et al., 2000). However, the climate impacts on cosmogenic radionuclides challenge the interpretation of cosmogenic radionuclides in terms of production rate variations. Consequently, to extract the production signal and derived GDM estimates, it is necessary to properly identify and remove the climate effects in cosmogenic radionuclide

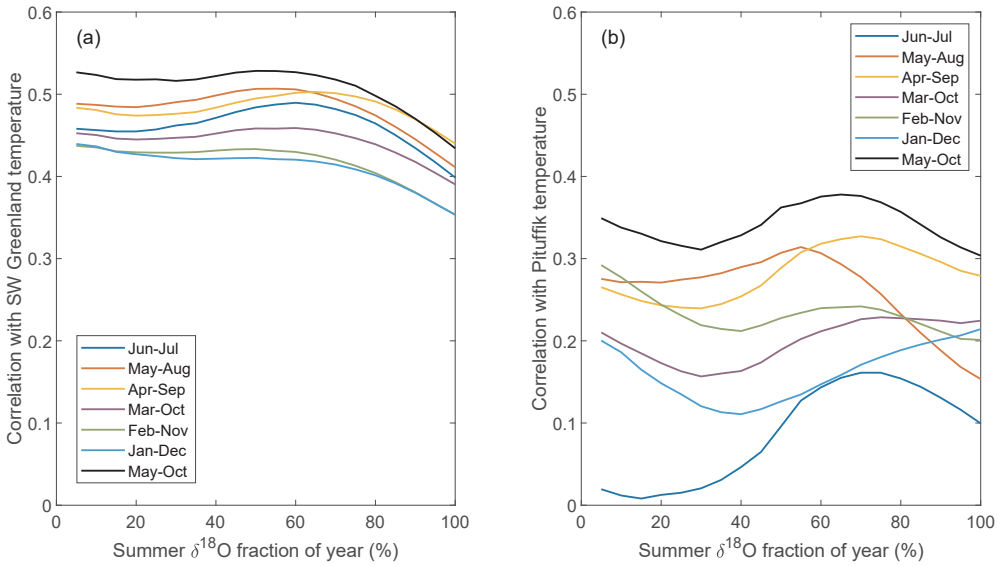

Figure 11. Correlation coefficients between averaged summer δ^{18}O data (depending on variously defined choices of summer δ^{18}O data) and measured temperature records of SW Greenland (a, period 1855-2004) and Pituffik (b, period 1949-2004) depending on variously defined choices of months for summer temperature averages (different lines). The solid black line is the best summer signal identified in paper I.

data. In paper IV we present a GDM reconstruction over the period from 11.7 ka to 108 ka BP (before present AD 1950) based on a new NEEM ^{10}Be record and published GRIP ^{10}Be and ^{36}Cl records. We find that the cosmogenic radionuclides records reflect a mixture of climate and production effects that require separation to evaluate changes in the GDM. To minimize climate-related variations on the radionuclide data, we applied a multi-linear correction method by removing common variability between ^{10}Be and ^{36}Cl and climate parameters (accumulation rates, δ^{18}O and chemical data) from the radionuclide records. The comparison of the resulting "climate corrected" radionuclide based GDM reconstruction with independent GDM records shows a good agreement. Furthermore, the "climate correction" leads to an improved agreement with independent GDM reconstructions compared to simply using radionuclide fluxes, validating our correction method to isolate production rate changes from ice core radionuclide records. Overall, with this linear correction method, it is possible to extend the GDM reconstructions based on cosmogenic radionuclides data from the ice cores back in time when there is a strong connection between climate and radionuclide data from the ice cores.

Paper V

Zheng, M., Sjolte, J., Adolphi, F., Aldahan, A., Possnert, G., Wu, M., Muscheler, R., 2020. Solar and Meteorological influences on seasonal atmospheric ^{7}Be in Europe for 1975 to 2018. In revision, Chemosphere.

Studying high-resolution air ^{7}Be concentrations can improve our understanding of the meteorological influences on beryllium transport processes. The advantage of ^{7}Be is that atmospheric ^{7}Be can be relatively easily measured by gamma spectrometry, and has been widely measured around the world in radiation monitoring programs with weekly resolutions (e.g. Kulan et al., 2006; Longo et al., 2019; Sangiorgi et al., 2019). Here, we investigate the seasonal atmospheric distribution of the naturally produced ^{7}Be in surface air over Europe between 40° N and 68° N during the period 1975–2018. The results suggest that inter-annual variability of ^{7}Be reflects production rates of the radionuclide induced by solar modulation of cosmic rays. To discuss the meteorological influences independent from the production influence, we calculate a production corrected record by subtracting the modelled ^{7}Be production rates from measured ^{7}Be. We found that each of investigated sites has its own combination of local meteorological factors that affect the inter-annual variability of seasonal ^{7}Be activity. The combination of the tropospheric production rates and meteorological parameters explain 24% to 79% of the seasonal ^{7}Be activity variance. We further apply a three-box model to study the influence of stratosphere-troposphere exchanges on ^{7}Be concentrations. The simulation supports that the seasonal cycle of ^{7}Be in Europe is controlled by two main factors: the changing height of the troposphere (seasonality of the tropopause height) and seasonal variations of stratosphere-troposphere exchanges.

5. Discussion

5.1 Seasonal signals in the NEEM ice core

Seasonal signals in the NEEM ice core are identified based on the strongest correlations between accumulation-weighted $\delta^{18}O$ and temperature data. The method assumes that $\delta^{18}O$ is reaching its maxima/minima values at the same time as temperature (Vinther et al., 2010). However, the timing of $\delta^{18}O$ extrema might shift by up to 2 months in some years (e.g. Bolzan and Strobel, 1994). To test how sensitive the result is to this assumption, we revisit this assumption by shifting the corresponding summer month one month forward when $\delta^{18}O$ maxima are hypothesized to occur. The $\delta^{18}O$ maxima are assumed to correspond to June/July month instead of July/August in paper I. It should be noted that this will result in a different selection of the corresponding months for the summer season. We focus on the summer season here because of the strong footprint of temperature in the summer $\delta^{18}O$ (paper I). The maximum correlation is again obtained when selecting 70% accumulation rate for summer season defined from April to September (Fig. 11). However, this correlation is lower than when the summer season is defined as May-Oct, which is the strongest summer signal identified in paper I (black line in Fig. 11). Therefore, it seems reasonable to assume that the $\delta^{18}O$ maxima co-occur when temperature reaches the maxima (July/August) as assumed in paper I, even though $\delta^{18}O$ extrema might shift by up to 2 months in some years.

5.2 Meteorological influences on Greenland ^{10}Be data

5.2.1 Greenland ^{10}Be over the neutron monitor period

To improve our understanding of the meteorological influences on the ^{10}Be deposition on Greenland, in this section we further assess the possible meteorological influences on all annually resolved ^{10}Be records from Greenland available for the neutron monitor period following the same method as in paper II: NGRIP ^{10}Be record (Berggren et al., 2009), Renland ^{10}Be record (Aldahan et al., 1998) and Das2 ^{10}Be record (Pedro et al., 2012) and compare them to the results obtained from the new NEEM data. The Dye3 record (Beer et al., 1990) is excluded since the data them after year 1958 have been identified as problematic (see paper III). The following discussion will focus on ^{10}Be concentrations for the reasons outlined in paper II. Noted that for all ^{10}Be records except for the NEEM record, the year is defined from January to December which is slightly different from the definition of the annual NEEM data in paper II and III (from November to October of the subsequent year). Here, we also define the year from January to December, however, this will have little influence since the following analysis of the NEEM data shows similar results as shown in paper II. Figure 12 shows the comparison between normalized ^{10}Be records and normalized global average production rates inferred from neutron monitor-based solar reconstructions (Herbst et al., 2017). We use the production model by Poluianov et al. (2016) with the local interstellar spectrum by Herbst et al. (2017). Except for the shorter Renland ^{10}Be record, all ^{10}Be records are significantly correlated with the global average production rates ($p<0.05$).

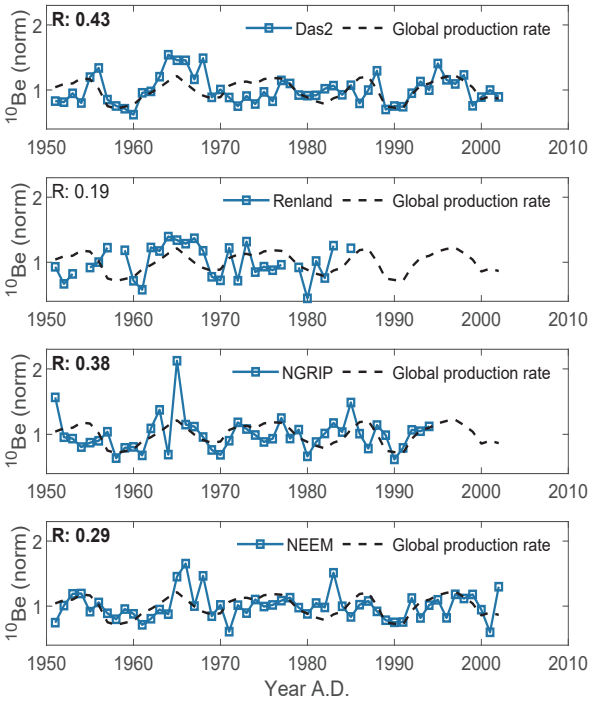

Figure 12. Comparison between ^{10}Be concentrations and modeled global average ^{10}Be production rates inferred from neutron monitor-based solar reconstructions (Herbst et al., 2017). All records are normalized by division through their mean for the common period 1951-1985. R-values in bold are significant at $p<0.05$ which are tested by a t-test adjusted for autocorrelation of the data (Hu et al., 2017). Data are linearly detrended before correlation analysis.

Table 2. Correlation coefficients between $^{10}Be_{conc\_climate}$ and accumulation rates from the corresponding ice cores, NAO and PNA index. Bold (underline) indicates significant correlations at $p<0.05$ ($p<0.1$). All data are linearly detrended before correlation analysis.

	Accumulation rates	NAO	PNA
Das2 $^{10}Be_{conc\_climate}$	**-0.54**	**-0.32**	0.10
Renland $^{10}Be_{conc\_climate}$	**-0.41**	0.04	-0.18
NGRIP $^{10}Be_{conc\_climate}$	**-0.44**	-0.02	-0.20
NEEM $^{10}Be_{conc\_climate}$	**-0.32**	-0.06	<u>0.24</u>

To better discuss the meteorological signal in the ^{10}Be records, we calculate the $^{10}Be_{conc\_climate}$ records, by subtracting modelled ^{10}Be production rates from ^{10}Be records and consider the residuals as the climate signal in ^{10}Be records (following the method in Paper II and V). First we compare $^{10}Be_{conc\_climate}$ records with the tropopause pressure extracted from the NCAR reanalysis data (Kalnay et al., 1996). All $^{10}Be_{conc\_climate}$ records are significantly correlated

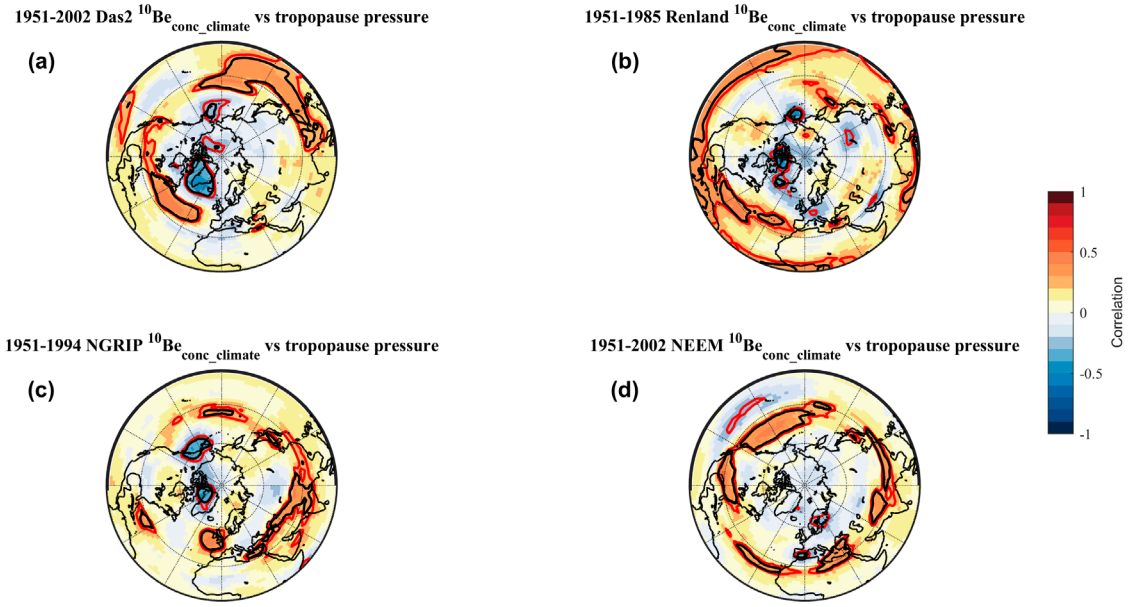

Figure 13. Spatial correlations between four Greenland $^{10}Be_{conc\_climate}$ records and the NCAR tropopause pressure data (Kalnay et al., 1996). Data are linearly detrended before correlation analysis. Red and black solid lines indicate significant correlations at the 90 and 95% confidence level (t-test).

with the tropopause pressure around mid-latitudes which are consistent with the conclusion in paper II, suggesting that tropopause pressure over 30°N represents an important factor influencing ^{10}Be concentrations in Greenland (Fig. 13).

$^{10}Be_{conc\_climate}$ records are also negatively correlated with the local tropopause pressure, suggesting the direct intrusion of the stratospheric ^{10}Be due to the tropopause folding. This negative correlation is not observed in the annually resolved NEEM record but in the summer NEEM data (shown in paper II). This stratospheric intrusion influence is further supported by the study of atmospheric ^{7}Be data from high Northern latitudes (e.g. Aldahan et al., 2008; Hernández-Ceballos et al., 2016). It should be mentioned that seasonal variations of the local tropopause height could also lead to changes of tropospheric beryllium, i.e. the higher local tropopause height the more formation of tropospheric beryllium (Ioannidou et al., 2014). However, this influence is reported less significant at high latitudes (e.g. polar regions) compared to mid latitudes (Hernández-Ceballos et al., 2016).

We further correlate $^{10}Be_{conc\_climate}$ records with the corresponding accumulation rates, North Atlantic Oscillation (NAO) and Pacific/North American (PNA) indexes (Table 2). The NAO and PNA indexes are calculated from the NCAR reanalysis data (Kalnay et al., 1996). The Das2 $^{10}Be_{conc\_climate}$ record is significantly correlated with the NAO index, which has already been reported in Pedro et al. (2012). The GCM study by Heikkilä and Smith (2013) suggests that the NAO is the main driver of the precipitation and ^{10}Be deposition in Greenland. Pedro et al. (2012) suggest that the Das2 ^{10}Be-NAO relationship can be explained by NAO influences on atmospheric processes (e.g. stratosphere - troposphere exchange) and the precipitation rate at the Das2 site. We do not find significant correlations between NAO and other $^{10}Be_{conc\_climate}$ records located in the central and northern Greenland. This may be due to the fact that central and northern Greenland are further away from the center of action of the North Atlantic Oscillation, hence, are less influenced by the NAO compared to the southern Greenland sites (Chylek et al., 2012). The study of δ^{18}O at the NEEM site also suggests less influence of the NAO pattern compared to southern Greenland (Steen-Larsen et al., 2011; Zheng et al., 2018). Only the NEEM $^{10}Be_{conc\_climate}$ is significantly correlated with PNA index ($p<0.1$). This suggests that the PNA circulation pattern may only influence northwest Greenland ^{10}Be through the modulation of aerosol transport to northern Greenland (Kang et al., 2015)

Interestingly, all $^{10}Be_{conc\_climate}$ records are significantly correlated with their corresponding accumulation rates. This correlation is not removed by calculating the ^{10}Be flux which shows significant positive correlation with the corresponding accumulation rate (for all ^{10}Be records). GCM studies suggest that the wet deposition is the dominant process for ^{10}Be deposition in Greenland for present-day climate (e.g. Heikkilä and Smith, 2013). In theory, for a site dominated by wet deposition one should expect that the concentration is independent of the local accumulation rate and the flux is expected to be accumulation rate dependent (Alley et al., 1995). In contrast, for a dominantly dry deposition site, significant negative correlations between ^{10}Be concentrations and accumulation rates should be expected. Pedro et al. (2012) suggest that for sites with very high accumulation rates (e.g. Das2 site), the large precipitation events can clean ^{10}Be from the atmosphere at the initial stage of precipitation while the later stage can dilute the ^{10}Be concentration in the snowpack. This can lead to a pattern resembling the

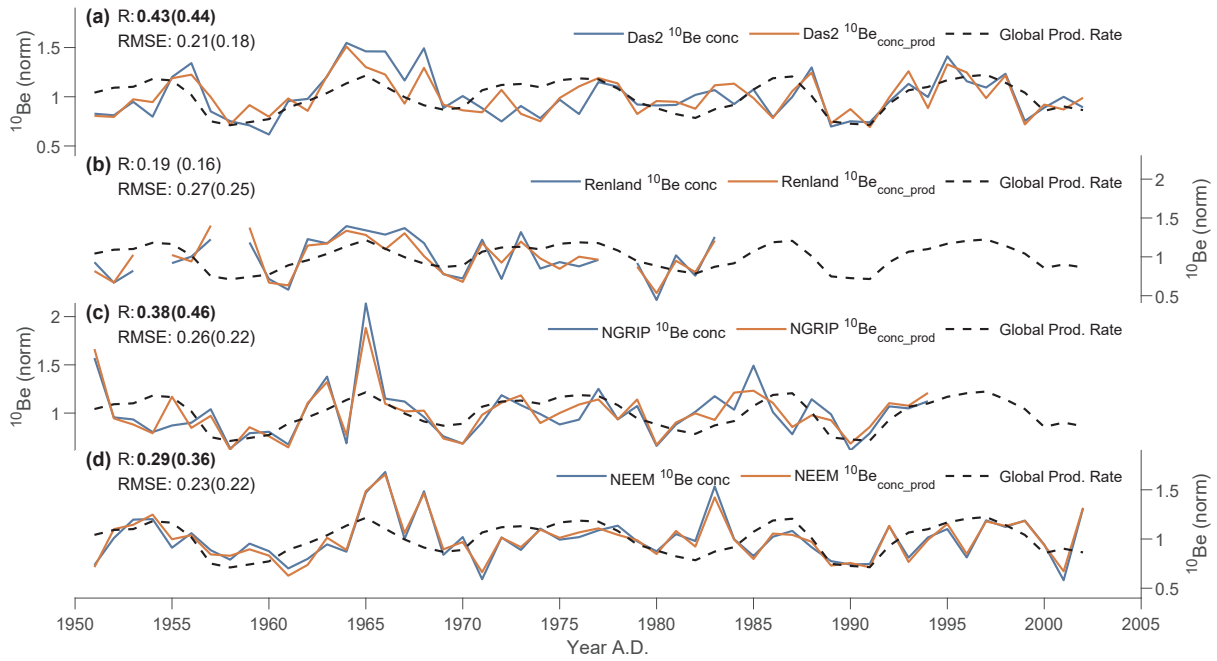

Figure 14. Comparison of the global average ^{10}Be production rate (dashed black), ^{10}Be concentrations (blue) and $^{10}Be_{conc\_prod}$ (red) for the Das2 (a), Renland (b), NGRIP (c) and NEEM (d) ice cores for the period 1951-2002. Values in the brackets are R and RMSE values between $^{10}Be_{conc\_prod}$ and global averaged production rates. The bold R-value indicates the significant result at p<0.05 tested by a t-test adjusted for autocorrelation of data (Hu et al., 2017). All data are linearly detrended before analysis.

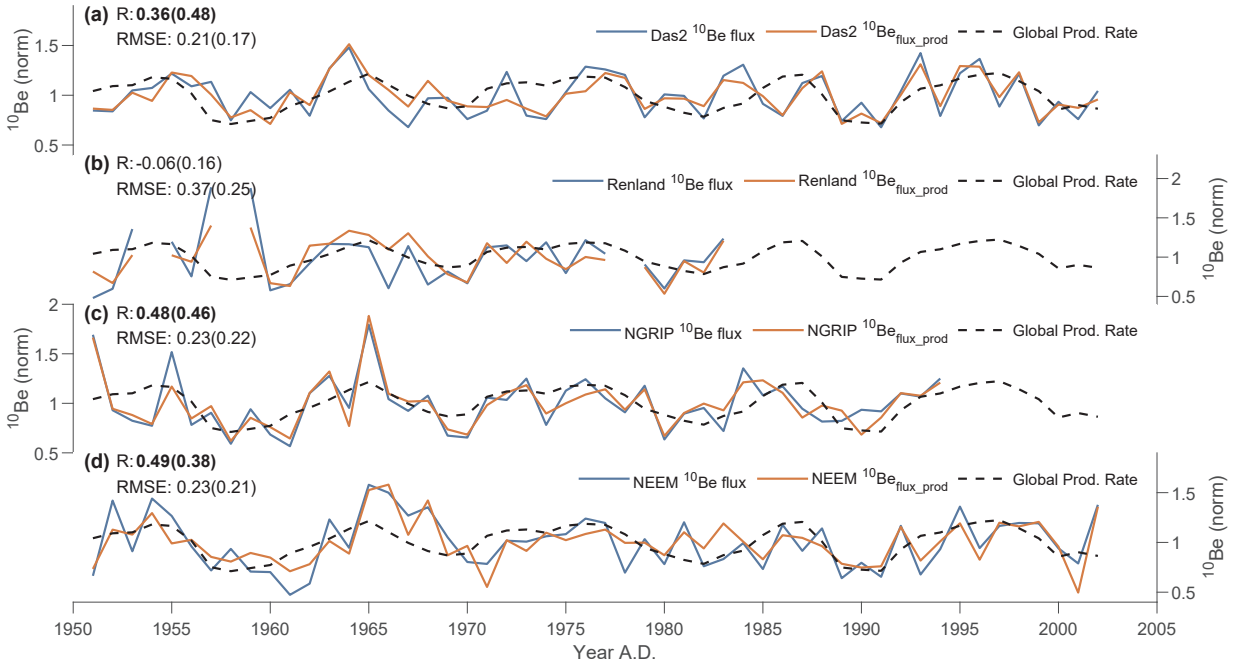

Figure 15. Comparison of the global averaged production rate (dashed black), ^{10}Be fluxes (blue) and $^{10}Be_{flux\_prod}$ (red) for Das2 (a), Renland (b), NGRIP (c) and NEEM (d) records for the period 1951-2002. Values in the brackets are R and RMSE values between $^{10}Be_{flux\_prod}$ and global averaged production rates. The bold R-value indicates the significant result at p<0.05 tested by a t-test adjusted for autocorrelation of data (Hu et al., 2017). All data are linearly detrended before analysis.

above-outlined dry deposition pattern even though ^{10}Be in this case is dominated by wet deposition. This dilution effect may be stronger at the Das2 site with high accumulation rates (0.90m/year) than at the NEEM site with relatively low accumulation rates (0.2m/year). We hypothesize that this can explain that the Das2 ^{10}Be record shows stronger negative correlation with the accumulation rate compared to the NEEM record (Table 2).

Since accumulation rates are negatively correlated with those ^{10}Be concentrations, a signal that cannot be removed by calculation of ^{10}Be fluxes, we subtract the linear relationship between accumulation rates and ^{10}Be concentrations from the ^{10}Be concentrations to see whether this can improve the relationship with modelled radionuclide production rates. The residual record is denoted as $^{10}Be_{conc\_prod}$. We only focus on accumulation rates in this model because other direct climate data usually are not

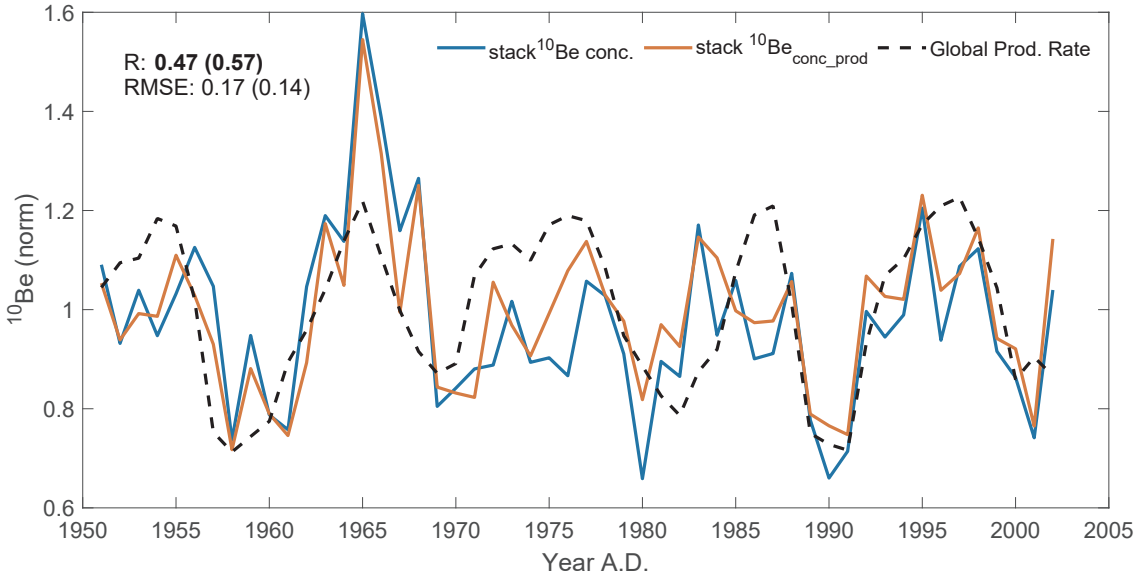

Figure 16. Comparison of the global average production rate (dashed black), the stack of ^{10}Be concentrations (blue) and the stack of ^{10}Be$_{conc_prod}$ (red) for the period 1951-2002 (see text). Values in the brackets are R and RMSE values between ^{10}Be$_{conc_prod}$ and global averaged production rates. The bold R-value indicates the significant result at p<0.05 tested by a t-test adjusted for autocorrelation of data (Hu et al., 2017). All data are linearly detrended before analysis.

available for the longer period (e.g. Holocene or glacial period). The results suggest that, by simply removing the linear accumulation rate dependency, we can partly reduce the differences between ^{10}Be data and theoretically expected production rates in terms of amplitudes (smaller RMSE, Fig. 14), although it may not always improve the correlation coefficients. The same conclusion also applies to the ^{10}Be flux by doing the corresponding analysis (Fig. 15). We further average those ^{10}Be$_{conc_prod}$ records (referred as stack ^{10}Be$_{conc_prod}$ record) to see whether the averaged record can enhance the production signal. The stack ^{10}Be$_{conc_prod}$ record shows higher correlation coefficient and lower RMSE value with the production rates than simply averaging the uncorrected ^{10}Be concentration records (Fig. 16). This result suggests that averaging climate-corrected ^{10}Be records are a better approach to enhance the production signal than simply averaging uncorrected ^{10}Be records. This is also suggested in paper IV when the averaged climate correction record shows smaller RMSE value with independent geomagnetic dipole moment reconstructions than simply averaging uncorrected ^{10}Be fluxes. Furthermore, this approach could be helpful when the calculation of the ^{10}Be flux does not completely remove the accumulation signal in ^{10}Be data. For example, in paper IV both GRIP ^{10}Be concentration and flux show significant correlations with accumulation rates for the Marine Isotope Stage 2-4 (11.7 ka – 71 ka BP).

Besides the above-discussed accumulation rate correction, previous studies have suggested the possibility of using chemical data such as sulfate and sodium measurements from the same core to evaluate the climate biases in ^{10}Be records (e.g. Adolphi and Muscheler, 2016; Miyake et al., 2019). Paper IV also indicates the potential of a better isolation of the production signal in ^{10}Be records by reducing the common signal with the accumulate rate and chemical ion data from the same ice core. To further validate this method, here we analyze two available published sub-annually resolved ^{10}Be and sulfate records from the Vostok and Dome C ice cores in Antarctica over the neutron monitor period (Baroni et al., 2011). The ^{10}Be and sulfate data are resampled to annual resolution using linear interpolation. The SO_4 record is log transformed for the subsequent analysis due to its logarithmical distribution. ^{10}Be concentrations from Dome C and Vostok show significant correlations with the corresponding sulfate concentrations (Fig. 17). Baroni et al. (2011) suggest that volcanic eruptions can enhance the aerosol sedimentation in the following years, thereby enhancing the stratospheric input of ^{10}Be-attached aerosol into troposphere, leading to increase of ^{10}Be depositions. To correct for this effect, Baroni et al. (2011) construct a linear model between Vostok ^{10}Be data and sulfate concentration for the volcanic eruption periods of Agung (about 1963-1968) and Pinatubo (about 1991-1998) and subtract this linear dependency from the ^{10}Be data only for that specific eruption period. However, this correction necessarily creates discontinuities and spurious jumps/artifacts at each volcano eruption-transition. Here we apply the linear correction for the whole period by linearly detrending the dependency between ^{10}Be and sulfate data (referred ^{10}Be$_{conc_SO4}$). The ^{10}Be$_{conc_SO4}$ records for Vostok and Dome C show higher correlations and lower RMSE values with the global averaged production rates than the original data (Fig. 18). Especially for the 1965-1970 period the high ^{10}Be concentration is largely removed. Via

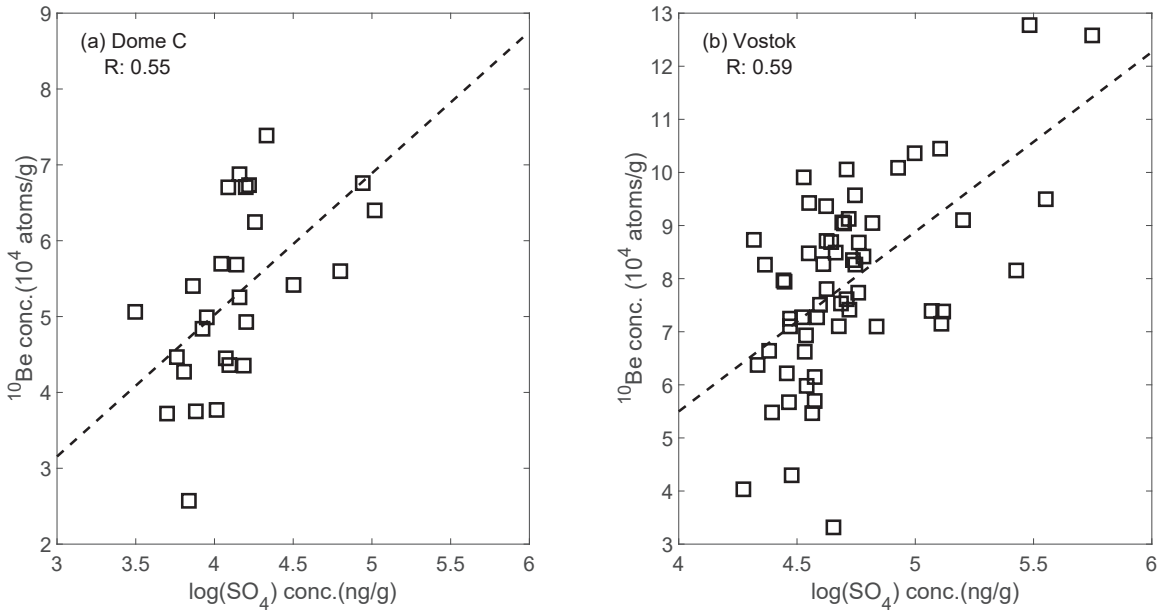

Figure 17. Correlations between SO_4 concentrations and ^{10}Be concentrations from Dome C (a, 1985-2011) and Vostok (b, 1951-2007) ice cores in Antarctica (Baroni et al., 2011). The SO_4 data are log transformed before correlations.

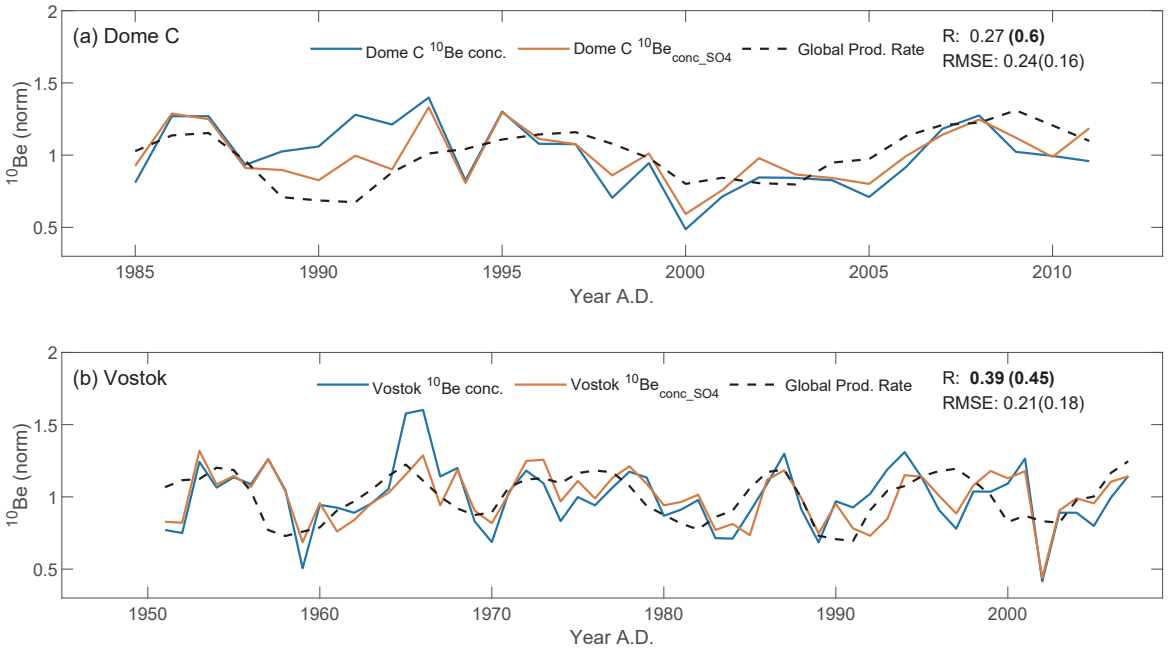

Figure 18. Comparison of the global averaged production rate (dashed black), ^{10}Be concentrations (blue) and ^{10}Be$_{conc_SO4}$ (red) records from Dome C (a, 1985-2011) and Vostok (b, 1951-2007) ice cores. Data are normalized by dividing through their mean. Values in the brackets are the ones between ^{10}Be$_{conc_SO4}$ and global averaged production rates. The bold R-value indicates the significant result at p<0.05 tested by a t-test adjusted for autocorrelation of data (Hu et al., 2017). All data are linearly detrended before analysis.

correlating with the NCAR tropopause pressure, we find that both ^{10}Be and SO_4 concentrations significantly correlate with the tropopause pressure over the mid-latitudes in the Southern Hemisphere (Fig. 19). This may indicate that the ^{10}Be-SO_4 relationship could possibly also reflect the common tropopause modulation influences on the ^{10}Be and SO_4 deposition in Antarctica.

Overall, we propose that by linearly detrending the common variances between climate or climate proxy data (e.g. accumulation rates, sulfate) and ^{10}Be, we can reduce the climate noise and enhance the ^{10}Be production signal. This method could be useful even when only the accumulation rate or ion data are available. It should be noted that such a correction could possibly remove the production (solar) variations that might be linked to the Greenland climate (e.g. Adolphi et al., 2014; Sturevik-Storm et al., 2014). However, this correction is expected to have little influence when focusing on the geomagnetic signal in ^{10}Be records because there is no convincing evidence suggesting a direct relationship between geomagnetic dipole moment and Greenland climate (e.g. Wagner et al.

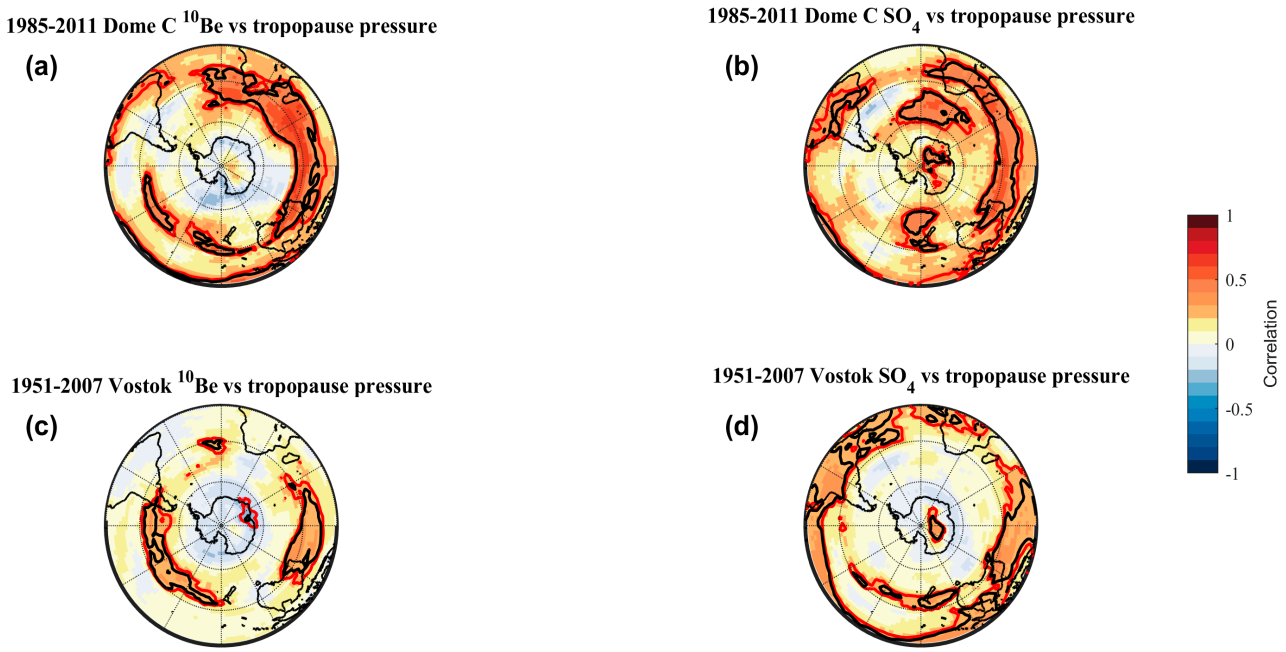

Figure 19. Correlation of ^{10}Be concentrations and SO_4 concentrations from Dome C (a-b, 1985-2011) and Vostok (c-d,1951-2007) ice cores with the NCAR tropopause pressure. All data are detrended and SO_4 data are log transformed before correlation analysis.

2001).

5.2.2 Comparing Greenland ^{10}Be to group sunspot numbers

In paper III, we find that even after correction of the Dye3 data problem, there are still some disagreements between solar reconstructions based on polar ^{10}Be records, which could be possibly attributed to the regional climate influences. Here we compare these solar reconstructions with the one based on group sunspot numbers (Svalgaard and Schatten, 2016) for the period 1611-1994. The group sunspot number data are transferred to a solar modulation record based on the model by Solanki et al. (2000) and Usoskin et al. (2002). The solar modulation function reconstruction based on Greenland ^{10}Be records shows a larger disagreement (RMSE=207) with the group sunspot numbers-based record compared to the Antarctic ^{10}Be record (RMSE=134) (Fig. 20). The Greenland-based reconstruction shows relative low values compared to the others (e.g. from 1700 to 1800 A.D.). In this section we study the possible climate causes for this disagreement in more detail. The group sunspot number based solar modulation function further are transferred to ^{10}Be production rates using the production model by Poluianov et al. (2016) with the local interstellar spectrum by Herbst et al. (2017). The geomagnetic data for the period 1611-1994 are from Muscheler et al. (2016) which combines the geomagnetic record from the geomagnetic model (Nilsson et al., 2014) and the modern values (Jackson et al., 2000; Thébault et al., 2015). Figure 21 shows the comparison between modelled global averaged production rates based on group sunspot numbers and the NGRIP and Dye3 ^{10}Be records covering this period. As discussed in paper III, the Dye3 data after 1958 are excluded from the analysis. Both Dye3 and NGRIP ^{10}Be records show significant correlations with modelled global averaged ^{10}Be production rates calculated from the group sunspot numbers (Fig. 21 a-b). The averaged record of Dye3 and NGRIP ^{10}Be data (referred as stack ^{10}Be), shows a higher correlation coefficient and a lower RMSE value compared to the individual ^{10}Be records (Fig. 21c). It should be noted that for some periods (e.g. around 1650) the ^{10}Be records show larger disagreements to the group sunspot number based- production rates. These differences cannot be removed by simply using a low pass-filter to filter out the "weather" noise. Furthermore, calculation of ^{10}Be fluxes did not lead to a better correlation or lower RMSE compared to using ^{10}Be concentrations.

We investigate a possible atmospheric circulation influence on Greenland ^{10}Be records by comparing these records with the winter NAO reconstruction by Sjolte et al. (2018). This NAO reconstruction, based on seasonally resolved d^{18}O data from Greenland ice cores and climate model simulations, preserves the amplitude of the observed year to year atmospheric variability prior to the instrumental period (Sjolte et al., 2018). The climate signal in ^{10}Be data (referred as $^{10}Be_{con\_climate}$) is obtained by subtracting the normalized production rate based on group sunspot number from the normalized ^{10}Be concentration.

The NAO is significantly correlated with the Dye3 $^{10}Be_{con\_climate}$ record (R: 0.14, p<0.05) but not with the NGRIP $^{10}Be_{con\_climate}$ (Figure 22 a-b). This analysis indicates that records from the Central and Northern Greenland (e.g. NGRIP record) are not significantly influenced

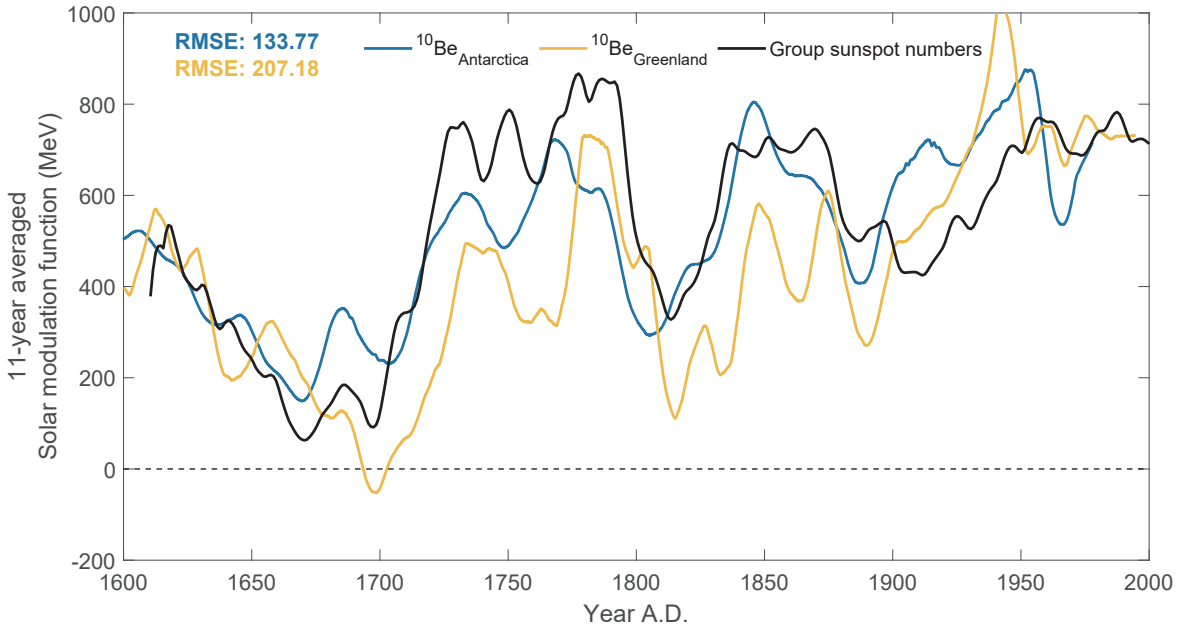

Figure 20. Solar modulation function reconstructions based on polar ^{10}Be data (paper III) and group sunspot numbers (Svalgaard and Schatten, 2016) for the period 1611-1994. ^{10}Be based reconstructions are calculated with the production-rate calculation from Poluianov et al. (2016) and geomagnetic-field data from Muscheler et al. (2016) which combines a geomagnetic model result (Nilsson et al., 2014) with modern values (Jackson et al., 2000; Thébault et al., 2015). Group sunspot numbers-based reconstruction is calculated following Solanki et al. (2000) and Usoskin et al. (2002). The RMSE is the root mean square error between polar ^{10}Be-based reconstructions and group sunspot numbers-based reconstruction.

by the NAO pattern compared to ^{10}Be from Southern Greenland (e.g. Dye3 record), supporting the discussion earlier that the NAO influences on ^{10}Be depositions in Greenland is site dependent (section 5.2.1). The stack record still shows significant correlation with the NAO (R: 0.13, $p<0.05$). However, it should be noted that even if there are correlations between Dye3 ^{10}Be and NAO, the circulation pattern can only explain less than 2% of the variance of the ^{10}Be record. Therefore, the results suggest that differences between Greenland ^{10}Be and modelled expected production rate may not be attributed to the influence of the NAO circulation pattern alone.

6. Summary and conclusions

The main focus of this thesis is to improve our understanding of the weather/climate influences on ^{10}Be data from ice cores and minimize such climate influences to improve ^{10}Be-based solar and geomagnetic field reconstructions. This is done by measuring and investigating the new ^{10}Be records from NEEM ice core and atmospheric ^{7}Be data in comparison to weather/climate data. The main conclusions and findings are summarized as follows:

- δ^{18}O at the NEEM site is found to be weakly influenced by the winter NAO. This has to be kept in mind when combining NEEM δ^{18}O records with other proxy data in circulation reconstructions.
- On multi-annual and longer timescales, the investigated seasonally resolved ^{10}Be and ^{7}Be records reflect the solar signal introduced by the solar modulation of the galactic cosmic rays.
- A method to better discuss the meteorological influence on ^{10}Be and ^{7}Be data is proposed by removing the expected modelled production rate from the measured data. This allows us to discuss the meteorological influences on ^{10}Be and ^{7}Be records independent from production influences.
- The tropopause over the mid-latitudes in the north hemisphere plays an important role for the ^{10}Be deposition at the investigated sites in Greenland.
- Linearly detrending the common variances (through linear or multi-linear models) between ^{10}Be records and identified weather/climate data or ice core proxy data helps to minimize the climate influences on ^{10}Be. The best results are obtained when individual ^{10}Be records where first climate-corrected and then stacked.
- With the linear correction method, geomagnetic field reconstruction based on cosmogenic radionuclide data from ice cores can be extended further back in time when there is a strong climate signal in the radionuclide data.
- The Dye3 ^{10}Be data are identified with unusual low

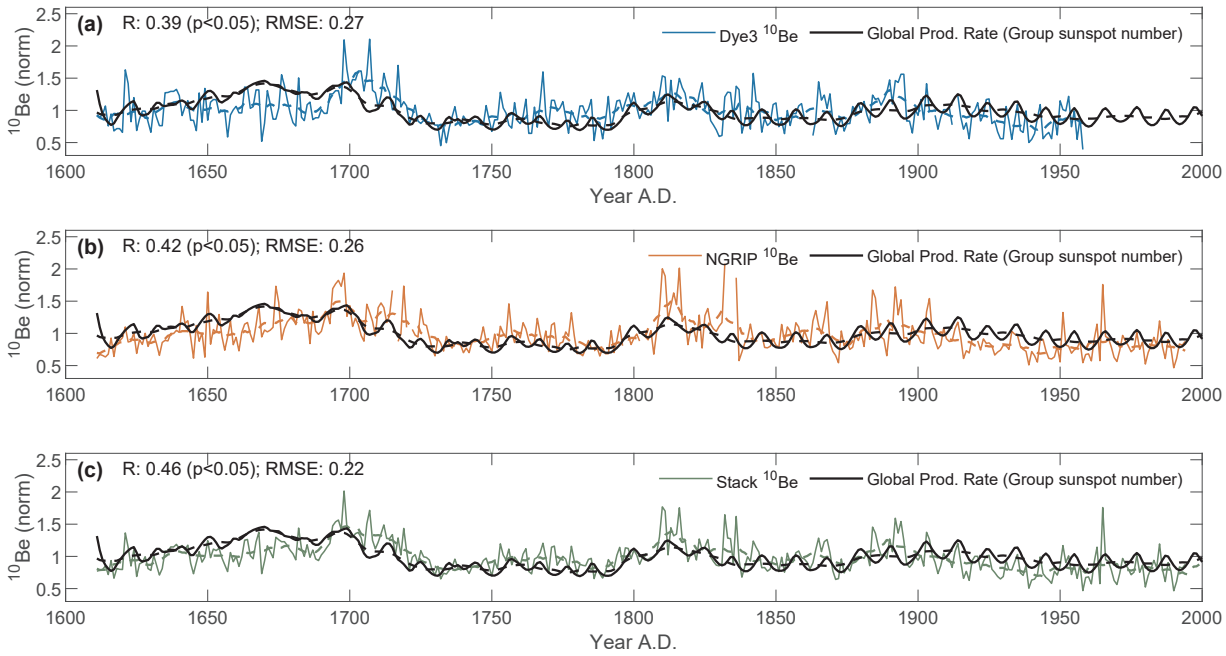

Figure 21. Comparison of global averaged ^{10}Be production rates inferred from the group sunspot number record and Dye3 ^{10}Be (a), NGRIP ^{10}Be (b) and averaged ^{10}Be (referred as "stack") concentration data. The data are normalized to the common period 1611-1958. The solid line is annual resolution while the dashed line is the 11-running mean.

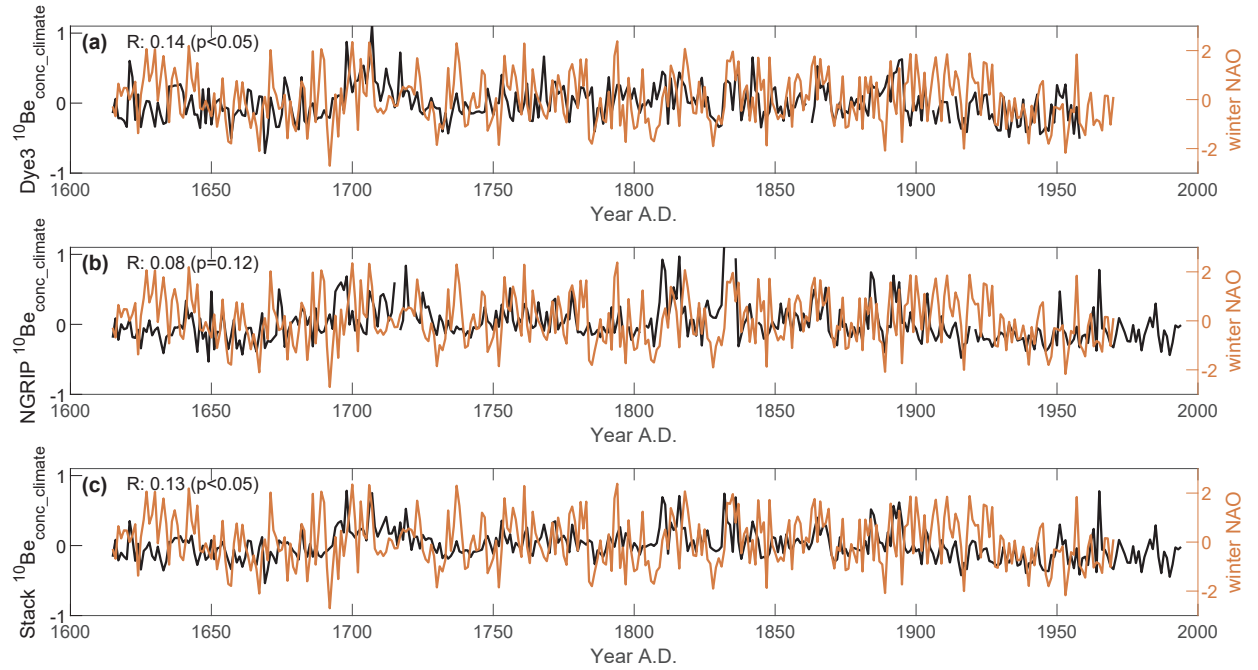

Figure 22. Comparison between $^{10}Be_{conc\_climate}$ records and the winter NAO reconstruction by Sjolte et al. (2018) for the period 1611-1994.

values after 1958 compared to the NGRIP and NEEM data, which is likely connected to a data problem instead of local weather influences. If uncorrected, this leads to a problem for solar activity reconstructions when connecting past ^{10}Be variations to absolute solar modulation function levels obtained from the neutron monitor data.

- The differences between solar reconstructions based on Greenland and Antarctic ^{10}Be records over last 2000 years are strongly reduced, after excluding the Dye3 ^{10}Be data after 1958. Consequently, the solar reconstruction from Greenland ^{10}Be no longer supports earlier claims of unusually high recent solar activity over the last 100 years.
- ^{10}Be data from polar regions and group sunspot numbers do not suggest a strong increase in solar activity for the 1937-1950 period questioning previous extensions of the neutron monitor data.
- The seasonal cycle of atmospheric ^{7}Be in Europe is controlled by two main factors: seasonal variations of the troposphere height and seasonal variations of the stratosphere-troposphere exchange.

Svensk sammanfattning

Solen är den viktigaste energikällan för jordens klimatsystem, men hur variationer i solens aktivitet påverkar klimatet är fortfarande oklart. Genom att studera förändringar i solens aktivitet bakåt i tiden kan vi bättre förstå vilken roll solen spelar för jordens klimat. Kosmogena radionuklider, såsom ^{10}Be i iskärnor, fungerar som utmärkta proxydata för att rekonstruera variationer i solaktivitet längre bakåt i tiden än vad som är möjligt med direkta observationer. Kosmogena nukleider skapas när kosmisk strålning interagerar med molekyler i jordens atmosfär. Produktionshastigheten (av t.ex. ^{10}Be) beror på variationer i styrkan av solens och jordens magnetfält som fungerar som ett skydd mot den kosmiska strålningen. Ett starkt magnetfält leder till mindre kosmiska strålning och en lägre produktion. Studier av kosmogena nukleider kan därför ge användbar information om förändringar av solaktivitet och jordens magnetfält bakåt i tiden. Tolkningen av ^{10}Be-data försvåras pga. bristande kunskap om hur olika processer i atmosfären påverkar mängden ^{10}Be som når den slutliga depositionsplatsen. Om ^{10}Be-data inte korrigeras för sådana klimatrelaterade faktorer kan det leda till fel i rekonstruktionerna av solens aktivitet och jordens magnetfält.

Målet med detta projekt är att öka vår förståelse av hur klimatrelaterade processer påverkar depositionen av 10-beryllium i Grönland med hjälp av analyser av högupplösta ^{10}Be- och ^{7}Be-data för att i sin tur förbättra rekonstruktioner av solaktivitet och jordens magnetfält. Här presenterar vi ett väldefinierat säsongsupplöst ^{10}Be-arkiv för perioden 1887-2002 från en borrkärna (NEEM07S1) genom de övre delarna av istäcket i nordvästra Grönland. Genom att analysera säsongsvariationer av syreisotoper (δ^{18}O) i NEEM-borrkärnan beräknar vi att 30% av snön ackumulerats under vinterhalvåret (november-april) och att 70% ackumulerats under sommarhalvåret (maj-oktober). Både sommar och vinter ^{10}Be-data återspeglar delvis den atmosfäriska produktionssignalen som i sin tur beror på solens modulering av galaktiska kosmiska strålar. Utöver denna solaktivitetsrelaterade signalen finner vi att tropopaustrycket över 30°N också representerar en viktig faktor som påverkar koncentrationen av ^{10}Be i NEEM-borrkärnan. ^{10}Be-koncentrationen på sommaren är i genomsnitt högre än på vintern, vilket kan förklaras av ett ökat stratosfärisk intrång av ^{10}Be under sommaren. Ett ökat stratosfäriskt intrång av beryllium-10 stöds av högupplösta studier av ^{7}Be i luftprover över Europa.

Genom jämförelser med ^{10}Be-data från andra grönländska iskärnor över de senaste 100 åren kan vi även konstatera att ^{10}Be-värdena från Dye3-iskärnan efter 1958 är ovanligt låga, vilket vi tolkar som ett dataproblem snarare än inverkan av meteorologiska variationer. Perioden med ovanligt låga ^{10}Be-värden i Dye3 kan skapa problem när radionuklidvariationerna normaliseras för att kopplas samman med direkta observationer av kosmisk strålning över de senaste 70 åren från markbaserade neutrondetektorer. Vi fann att skillnader mellan olika solaktivitetsrekonstruktioner baserade på iskärnor från Grönland och Antarktis delvis kan förklaras av detta dataproblem.

Slutligen presenterar vi en rekonstruktion av variationer i styrkan av jordens magnetfält från 108 000 till 11 700 år för nutid (AD 1950) baserat på nya ^{10}Be-data från NEEM-borrkärnan samt redan publicerade GRIP ^{10}Be- och ^{36}Cl-data. Vi undersöker möjligheten att korrigera kosmogena radionukliddata med hjälp av klimatproxydata och demonstrerar att även en enkel "klimatkorrigering" förbättrar korrelationen med oberoende magnetfältsrekonstruktioner jämfört med att använda okorrigerad radionukliddata. Detta resultat validerar användningen av kosmogena radionuklider i iskärnor för att rekonstruera variationer i jordens magnetfält bakåt i tiden, förutsatt att klimatpåverkan korrigerats för.

References

Abreu, J.A., Beer, J., Steinhilber, F., Christl, M., Kubik, P.W., 2012. ^{10}Be in Ice Cores and ^{14}C in Tree Rings: Separation of Production and Climate Effects. Space Science Reviews 176, 343-349.

Ackermann, M., Ajello, M., Allafort, A., Baldini, L., Ballet, J., Barbiellini, G., Baring, M.G., Bastieri, D., Bechtol, K., Bellazzini, R., Blandford, R.D., Bloom, E.D., Bonamente, E., Borgland, A.W., Bottacini, E., Brandt, T.J., Bregeon, J., Brigida, M., Bruel, P., Buehler, R., Busetto, G., Buson, S., Caliandro, G.A., Cameron, R.A., Caraveo, P.A., Casandjian, J.M., Cecchi, C., Çelik, Ö., Charles, E., Chaty, S., Chaves, R.C.G., Chekhtman, A., Cheung, C.C., Chiang, J., Chiaro, G., Cillis, A.N., Ciprini, S., Claus, R., Cohen-Tanugi, J., Cominsky, L.R., Conrad, J., Corbel, S., Cutini, S., Ammando, F., de Angelis, A., de Palma, F., Dermer, C.D., do Couto e Silva, E., Drell, P.S., Drlica-Wagner, A., Falletti, L., Favuzzi, C., Ferrara, E.C., Franckowiak, A., Fukazawa, Y., Funk, S., Fusco, P., Gargano, F., Germani, S., Giglietto, N., Giommi, P., Giordano, F., Giroletti, M., Glanzman, T., Godfrey, G., Grenier, I.A., Grondin, M.H., Grove, J.E., Guiriec, S., Hadasch, D., Hanabata, Y., Harding, A.K., Hayashida, M., Hayashi, K., Hays, E., Hewitt, J.W., Hill, A.B., Hughes, R.E., Jackson, M.S., Jogler, T., Jóhannesson, G., Johnson, A.S., Kamae, T., Kataoka, J., Katsuta, J., Knödlseder, J., Kuss, M., Lande, J., Larsson, S., Latronico, L., Lemoine-Goumard, M., Longo, F., Loparco, F., Lovellette, M.N., Lubrano, P., Madejski, G.M., Massaro, F., Mayer, M., Mazziotta, M.N., McEnery, J.E., Mehault, J., Michelson, P.F., Mignani, R.P., Mitthumsiri, W., Mizuno, T., Moiseev, A.A., Monzani, M.E., Morselli, A., Moskalenko, I.V., Murgia, S., Nakamori, T., Nemmen, R., Nuss, E., Ohno, M., Ohsugi, T., Omodei, N., Orienti, M., Orlando, E., Ormes, J.F., Paneque, D., Perkins, J.S., Pesce-Rollins, M., Piron, F., Pivato, G., Rainò, S., Rando, R., Razzano, M., Razzaque, S., Reimer, A., Reimer, O., Ritz, S., Romoli, C., Sánchez-Conde, M., Schulz, A., Sgrò, C., Simeon, P.E., Siskind, E.J., Smith, D.A., Spandre, G., Spinelli, P., Stecker, F.W., Strong, A.W., Suson, D.J., Tajima, H., Takahashi, H., Takahashi, T., Tanaka, T., Thayer, J.G., Thayer, J.B., Thompson, D.J., Thorsett, S.E., Tibaldo, L., Tibolla, O., Tinivella, M., Troja, E., Uchiyama, Y., Usher, T.L., Vandenbroucke, J., Vasileiou, V., Vianello, G., Vitale, V., Waite, A.P., Werner, M., Winer, B.L., Wood, K.S., Wood, M., Yamazaki, R., Yang, Z., Zimmer, S., 2013. Detection of the Characteristic Pion-Decay Signature in Supernova Remnants. Science 339, 807.

Adolphi, F., Muscheler, R., 2016. Synchronizing the Greenland ice core and radiocarbon timescales over the Holocene - Bayesian wiggle-matching of cosmogenic radionuclide records. Climate of the Past 12, 15-30.

Adolphi, F., Muscheler, R., Svensson, A., Aldahan, A., Possnert, G., Beer, J., Sjolte, J., Björck, S., Matthes, K., Thiéblemont, R., 2014. Persistent link between solar activity and Greenland climate during the Last Glacial Maximum. Nature Geoscience 7, 662-666.

Aldahan, A., Hedfors, J., Possnert, G., Kulan, A., Berggren, A.M., Söderström, C., 2008. Atmospheric impact on beryllium isotopes as solar activity proxy. Geophysical Research Letters 35.

Aldahan, A., Possnert, G., Johnsen, S.J., Clausen, H.B., Isaksson, E., Karlen, W., Hansson, M., 1998. Sixty year ^{10}Be record from Greenland and Antarctica. Proceedings of the Indian Academy of Sciences - Earth and Planetary Sciences 107, 139-147.

Alley, R., Finkel, R., Nishiizumi, K., Anandakrishnan, S., Shuman, C., Mershon, G., Zielinski, G., Mayewski, P.A., 1995. Changes in continental and sea-salt atmospheric loadings in central Greenland during the most recent deglaciation: model-based estimates. Journal of Glaciology 41, 503-514.

Bard, E., Raisbeck, G., Yiou, F., Jouzel, J., 2000. Solar irradiance during the last 1200 years based on cosmogenic nuclides. Tellus B 52, 985-992.

Baroni, M., Bard, E., Petit, J.-R., Magand, O., Bourlès, D., 2011. Volcanic and solar activity, and atmospheric circulation influences on cosmogenic ^{10}Be fallout at Vostok and Concordia (Antarctica) over the last 60 years. Geochimica et Cosmochimica Acta 75, 7132-7145.

Baumgartner, S., Beer, J., Masarik, J., Wagner, G., Meynadier, L., Synal, H.A., 1998. Geomagnetic Modulation of the ^{36}Cl Flux in the GRIP Ice

Core, Greenland. Science 279, 1330.

Beer, J., Blinov, A., Bonani, G., Finkel, R.C., Hofmann, H.J., Lehmann, B., Oeschger, H., Sigg, A., Schwander, J., Staffelbach, T., Stauffer, B., Suter, M., Wötfli, W., 1990. Use of ^{10}Be in polar ice to trace the 11-year cycle of solar activity. Nature 347, 164-166.

Beer, J., Finkel, R.C., Bonani, G., Gäggeler, H., Görlach, U., Jacob, P., Klockow, D., Langway, C.C., Neftel, A., Oeschger, H., Schotterer, U., Schwander, J., Siegenthaler, U., Suter, M., Wagenbach, D., Wölfli, W., 1991. Seasonal variations in the concentration of ^{10}Be, Cl^-, NO_3^-, SO_4^{2-}, H_2O_2, ^{210}Pb, ^{3}H, mineral dust, and $\delta^{18}O$ in greenland snow. Atmospheric Environment. Part A. General Topics 25, 899-904.

Beer, J., McCracken, K., Von Steiger, R., 2012. Cosmogenic Radionuclides: Theory and Applications in the Terrestrial and Space Environments. Springer Science and Business Media.

Berggren, A.-M., 2009. Influence of solar activity and environment on ^{10}Be in recent natural archives, Digital Comprehensive Summaries of Uppsala Dissertations from the Faculty of Science and Technology. Acta Universitatis Upsaliensis, Uppsala, p. 64.

Berggren, A.M., Beer, J., Possnert, G., Aldahan, A., Kubik, P., Christl, M., Johnsen, S.J., Abreu, J., Vinther, B.M., 2009. A 600-year annual ^{10}Be record from the NGRIP ice core, Greenland. Geophysical Research Letters 36.

Bolzan, J.F., Strobel, M., 1994. Accumulation-rate variations around Summit, Greenland. Journal of Glaciology 40, 56-66.

Burger, R.A., Potgieter, M.S., Heber, B., 2000. Rigidity dependence of cosmic ray proton latitudinal gradients measured by the Ulysses spacecraft: Implications for the diffusion tensor. Journal of Geophysical Research: Space Physics 105, 27447-27455.

Caballero-Lopez, R.A., 2004. Limitations of the force field equation to describe cosmic ray modulation. Journal of Geophysical Research 109.

Cauquoin, A., Raisbeck, G., Jouzel, J., Paillard, D., 2014. Use of ^{10}Be to Predict Atmospheric ^{14}C Variations during the Laschamp Excursion: High Sensitivity to Cosmogenic Isotope Production Calculations. Radiocarbon 56, 67-82.

Chylek, P., Folland, C., Frankcombe, L., Dijkstra, H., Lesins, G., Dubey, M., 2012. Greenland ice core evidence for spatial and temporal variability of the Atlantic Multidecadal Oscillation. Geophysical Research Letters 39.

Delaygue, G., Bekki, S., Bard, E., 2015. Modelling the stratospheric budget of beryllium isotopes. Tellus B: Chemical and Physical Meteorology 67.

Eddy, J.A., 1976. The maunder minimum. Science 192, 1189-1202.

Field, C.V., Schmidt, G.A., 2009. Model-based constraints on interpreting 20th century trends in ice core ^{10}Be. Journal of Geophysical Research 114.

Field, C.V., Schmidt, G.A., Koch, D., Salyk, C., 2006. Modeling production and climate-related impacts on ^{10}Be concentration in ice cores. Journal of Geophysical Research 111.

Heikkilä, U., 2007. Modeling of the atmospheric transport of the cosmogenic radionuclides ^{10}Be and ^{7}Be using the ECHAM5-HAM general circulation model.

Heikkilä, U., Beer, J., Feichter, J., 2008a. Modeling cosmogenic radionuclides ^{10}Be and ^{7}Be during the Maunder Minimum using the ECHAM5-HAM General Circulation Model. Atmospheric Chemistry and Physics 8, 2797-2809.

Heikkilä, U., Beer, J., Feichter, J., 2009. Meridional transport and deposition of atmospheric ^{10}Be. Atmospheric Chemistry and Physics 9, 515-527.

Heikkilä, U., Beer, J., Jouzel, J., Feichter, J., Kubik, P., 2008b. ^{10}Be measured in a GRIP snow pit and modeled using the ECHAM5-HAM general circulation model. Geophysical Research Letters 35.

Heikkilä, U., Smith, A.M., 2013. Production rate and climate influences on the variability of ^{10}Be deposition simulated by ECHAM5-HAM: Globally, in Greenland, and in Antarctica. Journal of Geophysical Research: Atmospheres 118, 2506-2520.

Herbst, K., Muscheler, R., Heber, B., 2017. The new local interstellar spectra and their influence on the production rates of the cosmogenic radionuclides ^{10}Be and ^{14}C. Journal of Geophysical Research: Space Physics 122, 23-34.

Hernández-Ceballos, M.A., Brattich, E., Cinelli, G., Ajtić, J., Djurdjevic, V., 2016. Seasonality of ^{7}Be concentrations in Europe and influence of tropopause height. Tellus B: Chemical and Physical Meteorology 68, 29534.

Hu, J., Emile-Geay, J., Partin, J., 2017. Correlation-based interpretations of paleoclimate data – where statistics meet past climates. Earth and Planetary Science Letters 459, 362-371.

Igarashi, Y., Hirose, K., Otsuji-Hatori, M., 1998. Beryllium-7 Deposition and Its Relation to Sulfate Deposition. Journal of Atmospheric Chemistry 29, 217-231.

Ioannidou, A., Vasileiadis, A., Melas, D., 2014. Time lag between the tropopause height and ^{7}Be activity concentrations on surface air. J Environ Radioact 129, 80-85.

Jackson, A., Jonkers Art, R.T., Walker Matthew, R., 2000. Four centuries of geomagnetic secular variation from historical records. Philosophical Transactions of the Royal Society of London. Series A: Mathematical, Physical and Engineering Sciences 358, 957-990.

Kalnay, E., Kanamitsu, M., Kistler, R., Collins, W., Deaven, D., Gandin, L., Iredell, M., Saha, S., White, G., Woollen, J., Zhu, Y., Chelliah, M., Ebisuzaki, W., Higgins, W., Janowiak, J., Mo, K.C., Ropelewski, C., Wang, J., Leetmaa, A., Reynolds, R., Jenne, R., Joseph, D., 1996. The NCEP/NCAR 40-Year Reanalysis Project. Bulletin of the American Meteorological Society 77, 437-472.

Kang, J.-H., Hwang, H., Hong, S.B., Hur, S.D., Choi, S.-D., Lee, J., Hong, S., 2015. Mineral dust and major ion concentrations in snowpit samples from the NEEM site, Greenland. Atmospheric Environment 120, 137-143.

Kovaltsov, G.A., Usoskin, I.G., 2010. A new 3D numerical model of cosmogenic nuclide ^{10}Be production in the atmosphere. Earth and Planetary Science Letters 291, 182-188.

Kulan, A., Aldahan, A., Possnert, G., Vintersved, I., 2006. Distribution of ^{7}Be in surface air of Europe. Atmospheric Environment 40, 3855-3868.

Lal, D., Peters, B., 1967a. Cosmic Ray Produced Radioactivity on the Earth, in: Sitte, K. (Ed.), Kosmische Strahlung II / Cosmic Rays II. Springer Berlin Heidelberg, Berlin, Heidelberg, pp. 551-612.

Lal, D., Peters, B., 1967b. Cosmic ray produced radioactivity on the Earth, Kosmische Strahlung II/Cosmic Rays II. Springer, pp. 551-612.

Longo, A., Bianchi, S., Plastino, W., 2019. tvf-EMD based time series analysis of ^{7}Be sampled at the CTBTO-IMS network. Physica A: Statistical Mechanics and its Applications 523, 908-914.

Masarik, J., Beer, J., 1999. Simulation of particle fluxes and cosmogenic nuclide production in the Earth's atmosphere. Journal of Geophysical Research: Atmospheres 104, 12099-12111.

Masson-Delmotte, V., Steen-Larsen, H.C., Ortega, P., Swingedouw, D., Popp, T., Vinther, B.M., Oerter, H., Sveinbjornsdottir, A.E., Gudlaugsdottir, H., Box, J.E., Falourd, S., Fettweis, X., Gallée, H., Garnier, E., Gkinis, V., Jouzel, J., Landais, A., Minster, B., Paradis, N., Orsi, A., Risi, C., Werner, M., White, J.W.C., 2015. Recent changes in north-west Greenland climate documented by NEEM shallow ice core data and simulations, and implications for past-temperature reconstructions. The Cryosphere 9, 1481-1504.

Mekhaldi, F., Muscheler, R., Adolphi, F., Aldahan, A., Beer, J., McConnell, J.R., Possnert, G., Sigl, M., Svensson, A., Synal, H.A., Welten, K.C., Woodruff, T.E., 2015. Multiradionuclide evidence for the solar origin of the cosmic-ray events of 774/5 and 993/4. Nat Commun 6, 8611.

Miyake, F., Horiuchi, K., Motizuki, Y., Nakai, Y., Takahashi, K., Masuda, K., Motoyama, H., Matsuzaki, H., 2019. ^{10}Be Signature of the Cosmic Ray Event in the 10th Century CE in Both Hemispheres, as Confirmed by Quasi-Annual ^{10}Be Data From the Antarctic Dome Fuji Ice Core. Geophysical Research Letters 46, 11-18.

Muscheler, R., Adolphi, F., Herbst, K., Nilsson, A., 2016. The Revised Sunspot Record in Comparison to Cosmogenic Radionuclide-Based Solar Activity Reconstructions. Solar Physics 291, 3025-3043.

Muscheler, R., Beer, J., Kubik, P.W., Synal, H.A., 2005. Geomagnetic field intensity during the last 60,000 years based on ^{10}Be and ^{36}Cl from the Summit ice cores and ^{14}C. Quaternary Science Reviews 24, 1849-1860.

Muscheler, R., Beer, J., Wagner, G., Laj, C., Kis-

sel, C., Raisbeck, G.M., Yiou, F., Kubik, P.W., 2004. Changes in the carbon cycle during the last deglaciation as indicated by the comparison of ^{10}Be and ^{14}C records. Earth and Planetary Science Letters 219, 325-340.

Muscheler, R.A., 2000. Nachweis von Änderungen im Kohlenstoffkreislauf durch Vergleich der Radionuklide ^{10}Be, ^{36}Cl und ^{14}C. Eidgenössische Technische Hochschule Zürich.

NEEM community members, 2013. Eemian interglacial reconstructed from a Greenland folded ice core. Nature 493, 489-494.

Nilsson, A., Holme, R., Korte, M., Suttie, N., Hill, M., 2014. Reconstructing Holocene geomagnetic field variation: new methods, models and implications. Geophysical Journal International 198, 229-248.

O'Brien, K., 1979. Secular variations in the production of cosmogenic isotopes in the Earth's atmosphere. Journal of Geophysical Research: Space Physics 84, 423-431.

O'Hare, P., Mekhaldi, F., Adolphi, F., Raisbeck, G., Aldahan, A., Anderberg, E., Beer, J., Christl, M., Fahrni, S., Synal, H.A., Park, J., Possnert, G., Southon, J., Bard, E., Team, A., Muscheler, R., 2019. Multiradionuclide evidence for an extreme solar proton event around 2,610 B.P. (approximately 660 BC). Proc Natl Acad Sci U S A 116, 5961-5966.

Organization, W.M., 1992. International meteorological vocabulary. Secretariat of the World Meteorolog. Organization.

Pedro, J.B., Heikkilä, U.E., Klekociuk, A., Smith, A.M., van Ommen, T.D., Curran, M.A.J., 2011a. Beryllium-10 transport to Antarctica: Results from seasonally resolved observations and modeling. Journal of Geophysical Research: Atmospheres 116.

Pedro, J.B., McConnell, J.R., van Ommen, T.D., Fink, D., Curran, M.A.J., Smith, A.M., Simon, K.J., Moy, A.D., Das, S.B., 2012. Solar and climate influences on ice core ^{10}Be records from Antarctica and Greenland during the neutron monitor era. Earth and Planetary Science Letters 355-356, 174-186.

Pedro, J.B., Smith, A.M., Simon, K.J., van Ommen, T.D., Curran, M.A.J., 2011b. High-resolution records of the beryllium-10 solar activity proxy in ice from Law Dome, East Antarctica: measurement, reproducibility and principal trends. Climate of the Past 7, 707-721.

Poluianov, S.V., Kovaltsov, G.A., Mishev, A.L., Usoskin, I.G., 2016. Production of cosmogenic isotopes ^{7}Be, ^{10}Be,^{14}C, ^{22}Na, and ^{36}Cl in the atmosphere: Altitudinal profiles of yield functions. Journal of Geophysical Research: Atmospheres 121, 8125-8136.

Raisbeck, G.M., Yiou, F., Fruneau, M., Loiseaux, J.M., Lieuvin, M., Ravel, J.C., 1981. Cosmogenic ^{10}Be/^{7}Be as a probe of atmospheric transport processes. Geophysical Research Letters 8, 1015-1018.

Sangiorgi, M., Hernández Ceballos, M.A., Iurlaro, G., Cinelli, G., de Cort, M., 2019. 30 years of European Commission Radioactivity Environmental Monitoring data bank (REMdb) – an open door to boost environmental radioactivity research. Earth System Science Data 11, 589-601.

Schupbach, S., Fischer, H., Bigler, M., Erhardt, T., Gfeller, G., Leuenberger, D., Mini, O., Mulvaney, R., Abram, N.J., Fleet, L., Frey, M.M., Thomas, E., Svensson, A., Dahl-Jensen, D., Kettner, E., Kjaer, H., Seierstad, I., Steffensen, J.P., Rasmussen, S.O., Vallelonga, P., Winstrup, M., Wegner, A., Twarloh, B., Wolff, K., Schmidt, K., Goto-Azuma, K., Kuramoto, T., Hirabayashi, M., Uetake, J., Zheng, J., Bourgeois, J., Fisher, D., Zhiheng, D., Xiao, C., Legrand, M., Spolaor, A., Gabrieli, J., Barbante, C., Kang, J.H., Hur, S.D., Hong, S.B., Hwang, H.J., Hong, S., Hansson, M., Iizuka, Y., Oyabu, I., Muscheler, R., Adolphi, F., Maselli, O., McConnell, J., Wolff, E.W., 2018. Greenland records of aerosol source and atmospheric lifetime changes from the Eemian to the Holocene. Nat Commun 9, 1476.

Sjolte, J., Sturm, C., Adolphi, F., Vinther, B.M., Werner, M., Lohmann, G., Muscheler, R., 2018. Solar and volcanic forcing of North Atlantic climate inferred from a process-based reconstruction. Climate of the Past 14, 1179-1194.

Solanki, S.K., Schüssler, M., Fligge, M., 2000. Evolution of the Sun's large-scale magnetic field since the Maunder minimum. Nature 408, 445-447.

Steen-Larsen, H.C., Masson-Delmotte, V., Sjolte,

J., Johnsen, S.J., Vinther, B.M., Bréon, F.M., Clausen, H.B., Dahl-Jensen, D., Falourd, S., Fettweis, X., Gallée, H., Jouzel, J., Kageyama, M., Lerche, H., Minster, B., Picard, G., Punge, H.J., Risi, C., Salas, D., Schwander, J., Steffen, K., Sveinbjörnsdóttir, A.E., Svensson, A., White, J., 2011. Understanding the climatic signal in the water stable isotope records from the NEEM shallow firn/ice cores in northwest Greenland. Journal of Geophysical Research 116.

Steinhilber, F., Abreu, J.A., Beer, J., Brunner, I., Christl, M., Fischer, H., Heikkila, U., Kubik, P.W., Mann, M., McCracken, K.G., Miller, H., Miyahara, H., Oerter, H., Wilhelms, F., 2012. 9,400 years of cosmic radiation and solar activity from ice cores and tree rings. Proc Natl Acad Sci U S A 109, 5967-5971.

Stocker, T.F., Qin, D., Plattner, G.-K., Tignor, M., Allen, S.K., Boschung, J., Nauels, A., Xia, Y., Bex, B., Midgley, B., 2013. IPCC, 2013: climate change 2013: the physical science basis. Contribution of working group I to the fifth assessment report of the intergovernmental panel on climate change. Cambridge University Press.

Stone, E.C., Cummings, A.C., McDonald, F.B., Heikkila, B.C., Lal, N., Webber, W.R., 2013. Voyager 1 Observes Low-Energy Galactic Cosmic Rays in a Region Depleted of Heliospheric Ions. Science 341, 150.

Sturevik-Storm, A., Aldahan, A., Possnert, G., Berggren, A.M., Muscheler, R., Dahl-Jensen, D., Vinther, B.M., Usoskin, I., 2014. ^{10}Be climate fingerprints during the Eemian in the NEEM ice core, Greenland. Sci Rep 4, 6408.

Svalgaard, L., Schatten, K.H., 2016. Reconstruction of the Sunspot Group Number: The Backbone Method. Solar Physics 291, 2653-2684.

Thébault, E., Finlay, C.C., Alken, P., Beggan, C.D., Canet, E., Chulliat, A., Langlais, B., Lesur, V., Lowes, F.J., Manoj, C., Rother, M., Schachtschneider, R., 2015. Evaluation of candidate geomagnetic field models for IGRF-12. Earth, Planets and Space 67 (1).

Usoskin, I.G., Mursula, K., Solanki, S.K., Schüssler, M., Kovaltsov, G.A., 2002. A physical reconstruction of cosmic ray intensity since 1610. Journal of Geophysical Research: Space Physics 107, SSH 13-11-SSH 13-16.

Usoskin, I.G., Field, C.V., Schmidt, G.A., Leppänen, A.-P., Aldahan, A., Kovaltsov, G.A., Possnert, G., Ungar, R.K., 2009. Short-term production and synoptic influences on atmospheric ^{7}Be concentrations. Journal of Geophysical Research 114.

Usoskin, I.G., Solanki, S.K., Schussler, M., Mursula, K., Alanko, K., 2003. Millennium-scale sunspot number reconstruction: evidence for an unusually active sun since the 1940s. Phys Rev Lett 91, 211101.

Vinther, B.M., Jones, P.D., Briffa, K.R., Clausen, H.B., Andersen, K.K., Dahl-Jensen, D., Johnsen, S.J., 2010. Climatic signals in multiple highly resolved stable isotope records from Greenland. Quaternary Science Reviews 29, 522-538.

Vogt, S., Herzog, G.F., Reedy, R.C., 1990. Cosmogenic nuclides in extraterrestrial materials. Reviews of Geophysics 28, 253-275.

Vonmoos, M., Beer, J., Muscheler, R., 2006. Large variations in Holocene solar activity: Constraints from ^{10}Be in the Greenland Ice Core Project ice core. Journal of Geophysical Research 111.

Wagner, G., Beer, J., Masarik, J., Muscheler, R., Kubik, P.W., Mende, W., Laj, C., Raisbeck, G.M., Yiou, F., 2001a. Presence of the Solar de Vries Cycle (~205 years) during the Last Ice Age. Geophysical Research Letters 28, 303-306.

Wagner, G., Laj, C., Beer, J., Kissel, C., Muscheler, R., Masarik, J., Synal, H.-A., 2001b. Reconstruction of the paleoaccumulation rate of central Greenland during the last 75 kyr using the cosmogenic radionuclides ^{36}Cl and ^{10}Be and geomagnetic field intensity data. Earth Planet. Sc. Lett. 193, 515-521.

Wagner, G., Masarik, J., Beer, J., Baumgartner, S., Imboden, D., Kubik, P.W., Synal, H.A., Suter, M., 2000. Reconstruction of the geomagnetic field between 20 and 60 kyr BP from cosmogenic radionuclides in the GRIP ice core. Nuclear Instruments and Methods in Physics Research Section B: Beam Interactions with Materials and Atoms 172, 597-604.

Webber, W.R., Higbie, P.R., 2010. What Voyager cosmic ray data in the outer heliosphere tells us about ^{10}Be production in the Earth's polar atmosphere in the recent past. Journal of Geo-

physical Research: Space Physics 115.

Yiou, F., Raisbeck, G.M., Baumgartner, S., Beer, J., Hammer, C., Johnsen, S., Jouzel, J., Kubik, P.W., Lestringuez, J., Stiévenard, M., Suter, M., Yiou, P., 1997. Beryllium 10 in the Greenland Ice Core Project ice core at Summit, Greenland. Journal of Geophysical Research: Oceans 102, 26783-26794.

Zheng, M., Sjolte, J., Adolphi, F., Vinther, B.M., Steen-Larsen, H.C., Popp, T.J., Muscheler, R., 2018. Climate information preserved in seasonal water isotope at NEEM: relationships with temperature, circulation and sea ice. Climate of the Past 14, 1067-1078.